1T

[redacted]

NATIONAL AERONAUTICS AND SPACE ADMINISTRATION

TECHNICAL MEMORANDUM X-636

PRELIMINARY PERFORMANCE ANALYSIS OF AIR LAUNCHING MANNED ORBITAL VEHICLES*

H
2
2
9

By Donald R. Bellman and Harold P. Washington

SUMMARY

A preliminary performance analysis was made to determine the capability of large subsonic and supersonic bombers for air launching manned hypersonic and satellite vehicles. The bombers considered now exist or are being developed in the United States. Four booster configurations were used in the calculations, with a winged vehicle of the Dyna-Soar type as the payload. Comparisons were made on the basis of vacuum specific impulse, burnout velocity, ratio of payload weight to launch-package gross weight, and structural weight.

The study showed that booster packages weighing no more than 200,000 pounds are capable of accelerating a 10,000-pound winged vehicle to orbital velocity after being launched eastward from a subsonic bomber, if a vacuum specific impulse of about 335 seconds can be achieved in the booster engines.

It was also found that a 1-percent variation in vacuum specific impulse from a nominal value of 320 seconds results in approximately a 1-percent variation in burnout velocity; whereas, an increase to 6 percent in the ratio of payload weight to launch-package gross weight from a nominal value of 5 percent decreases the burnout velocity by 1,400 feet per second.

It was determined also that the high drag of the booster package required to fit the supersonic-launch airplane offsets the performance advantage of launching supersonically rather than subsonically.

[redacted]d.

[redacted]

INTRODUCTION

The use of winged recoverable vehicles propelled by efficient air-breathing engines as first-stage boosters for hypersonic and satellite vehicles has considerable merit, ranging from reduced booster cost when a large number of launches are to be made to increased operational versatility. The use of this technique for launching upper-atmosphere sounding rockets has been frequently advocated. A discussion of the technique is presented in references 1 and 2. Launching a body into an earth orbit by such means was proposed in 1956 by A. C. Robotti, who based his calculations on an F-102 airplane (ref. 3). Air launching is also the objective of the more recent Project Caleb, conducted by the U. S. Navy, in which F4D and F4H airplanes are used (ref. 4).

H
2
2
9

For many years the air-launching technique was used to launch the X-1, X-2, and D-558-II aircraft and is now being used with the X-15 research airplanes. The resultant gains in performance and operational safety have been appreciable. To air-launch manned satellite vehicles, however, will require much greater launch-package weight. Some analysts have proposed the construction of large, specially built airplanes propelled by turbojet and ram-jet engines for boosting satellite vehicles of such size that they could be manned (refs. 5 and 6). Because of the enormous cost and the time that would be required to develop such airplanes, it is believed expedient to explore the capabilities of the larger bombers that now exist or are being developed in the United States. Presented in this paper are the results of a preliminary analytical study of the performance of satellite vehicles launched from two of these bombers. Similar studies have also been made by other investigators (ref. 7, for example).

In the investigation, most of the launches were made at a high subsonic Mach number; however, to show the effect of launch speed and altitude a few launches were made at a Mach number of 3. Altitudes were chosen that were appropriate to the speed and type of airplane being considered. Launch-package weights ranged up to 200,000 pounds using four different booster configurations. Although a payload weight of 10,000 pounds was used for most of the calculations, lighter and heavier weights were also investigated.

The launch airplanes imposed limitations on the selection of propellants for the booster engines. The gross-weight take-off limit precluded the use of solid propellants because their lower vacuum specific impulse made the weight requirement too high. The use of cryogenic propellants which require additional propellant and tanks within the launch airplane for top-off purposes was also excluded because of weight restrictions. Liquid hydrog[redacted]ed because of volume requirements. The study, th[redacted] use of nitrogen tetroxide and mixed hydrazine fuel as the propellant. A range of vacuum specific impulse from 300 seconds to 340 seconds was chosen in order to cover the practical values of this propellant combination and to show the effect of vacuum specific impulse on vehicle performance.

Calculations were made at the NASA Flight Research Center, Edwards, Calif. An IBM 650 digital computer was used with a program that considered the curvature of the earth, but not the earth's rotation.

H
2
2
9

SYMBOLS

a_X	longitudinal acceleration, g units
C_D	drag coefficient, based on a reference area of 330 sq ft
C_{L_α}	lift-coefficient variation with angle of attack
D	drag, lb
F	thrust, lb
g	local acceleration of gravity, ft/sec^2
g_v	centripetal acceleration, ft/sec^2
h	altitude, ft
$\dot{h}$	rate of change of altitude with time, ft/sec
I_{sp}	vacuum specific impulse, sec
L	lift, lb
M	Mach number
P	ambient pressure, lb/sq ft
q	dynamic pressure, lb/sq ft
r	radius of the earth, ft
S	total wing area, sq ft
t	time, sec

[redacted]

V velocity, ft/sec

$\dot{V}$ rate of change of velocity with time, ft/sec^2

ΔV incremental change in velocity, ft/sec

W vehicle weight, lb

α angle of attack, deg

γ flight-path angle, deg

$\dot{\gamma}$ rate of change of flight-path angle with time, deg/sec

ρ atmospheric density, slugs/cu ft

Subscripts:

0 sea-level condition

bo burnout

vac vacuum

H 2 2 9

CONFIGURATIONS

If a launch vehicle-booster-payload package, utilizing a prescribed payload and an existing bomber, is to be compatible, various modifications to the bomber will be necessary and the booster must be designed to fit both the bomber and the payload. With launch-package weights approaching those of the launch vehicle, positioning of the center of gravity is very important, and, because the payload will be manned, access to the cockpit is highly desirable. These factors have been considered in this study. An artist's conception of a subsonic bomber carrying one of the payload-booster combinations is shown in figure 1.

Payload

The payload used in this study was a winged vehicle of the Dyna-Soar type, having an assumed wing area of 330 square feet. A lifting payload was selected because it represented the more difficult booster-design problem. A nonlifting payload would have slightly greater performance capability because of reduced drag and increased propellant mass ratio as a result of less demanding stabilizing-fin requirements.

[redacted]

For most of the calculations a payload weighing 10,000 pounds was used. A few calculations were made using 5,000-pound and 15,000-pound payloads to determine the effect of payload weight.

Boosters

The four basic booster configurations used to perform the calculations are designated as types A, B, C, and D. Variations of the boosters are indicated by numerical subscripts, for example A_1. Physical data on the boosters are presented in table I. Each booster was equipped with sufficient fin area to make the booster-payload combination neutrally stable at launch. All of the fins were considered fixed, since it was assumed that a jet attitude-control system was in operation at launch.

H229

A drawing of the type A boosters with fins attached is shown in figure 2. These boosters were assumed to be single stage and to have three simultaneously firing rocket engines of 100,000 pounds vacuum thrust each.

The type B boosters were of the two-stage tandem type, as shown in figure 3. These boosters used three engines, two during the first stage and the remaining one for second-stage operation. Each of the three engines produced a vacuum thrust of 150,000 pounds.

Figure 4 and figure 5 show the type C and type D booster configurations, respectively. These configurations were also equipped with fins to make the vehicle neutrally stable at launch. Both configurations used three engines, two during the first-stage operation and the remaining one for second-stage operation. Each engine of both configurations produced a vacuum thrust of 150,000 pounds. Placement of the payload differed between the type C and type D configuration. For the type C configuration, the payload was placed ahead of the cluster of boosters; for the type D configuration, the payload was placed on top of the booster cluster.

Because of the specific configurations of the launch airplanes selected, the A, B, and C types would be most suitable for the subsonic-launch airplane and the D type for the supersonic-launch airplane. It would be possible, however, to devise a D-type configuration that could be used with both launch airplanes. This design would increase versatility for a single-booster development, but decrease the performance capabilities from the subsonic launch.

Booster volumes were based on the use of nitrogen tetroxide and mixed hydrazine fuel as the propellant. This combination has an average density of 75 pounds per cubic foot. For most of the calculations, the

[redacted]

basic booster structure was assumed to be 4 percent of the combined weight of the structure and the fuel. In a few instances, values of 2 percent and 8 percent were used. The fins were assumed to weigh an additional 6 pounds per square foot. The 100,000-pound-thrust and 150,000-pound-thrust engines were assumed to weigh 1,250 pounds and 1,900 pounds, respectively. The chosen propellant combination has a theoretical vacuum specific impulse of about 330 seconds, with a 40 to 1 expansion nozzle. In the calculations, vacuum specific-impulse values of 300 seconds, 320 seconds, and 340 seconds were used to show the effect of the variable on performance. H229

Carrier Airplanes

None of the proposed launch packages will fit completely in the bomb bay of either the subsonic or the supersonic carrier airplane being considered. However, for this study the packages are designed so that required modifications to the carrier airplanes would involve only the landing gear and nonstructural components of the fuselage and, possibly, strengthening of the attach points.

For most of the launch-package configurations, the landing gear of the subsonic-launch airplane would have to be extended and the tread widened, which would make it impractical to retract the landing gear in flight. In the computations the launch speed and altitude were reduced from the normal cruise conditions to account for the increased drag caused by the launch package and the extended landing gear.

It was assumed that the supersonic-launch airplane would have sufficient excess power to compensate for the added drag of the launch package, but streamlined fairings would have to be added.

COMPUTATION METHOD

The trajectories used for this preliminary analytical study were calculated on an IBM 650 digital computer by using the Runge-Kutta method of numerical integration. The equations of motion solved assumed a nonrotating spherical earth. The two-dimensional equations of motion then are

[redacted]

[redacted]

$$\dot{V} = g_0\left(\frac{F \cos \alpha - D}{W} - \frac{g \sin \gamma}{g_0}\right)$$

$$\dot{\gamma} = \frac{g_0}{V}\left(\frac{F \sin \alpha - L}{W} - \frac{g_V}{g_0} \cos \gamma\right)$$

$$\dot{h} = V \sin \gamma$$

H
2
2
9

where

$$g_V = g - \frac{V^2}{r + h}$$

$$L = \frac{\rho V^2 C_{L_\alpha} \alpha S}{2}$$

$$D = \frac{\rho V^2 C_D S}{2}$$

$$F = F_{vac} - \left(F_{vac} - F_0\right) \frac{P}{P_0}$$

During the numerical-integration process, the required values of pressure and density were obtained from a series of curve fits for the ARDC model atmosphere (ref. 8). Each condition was computed by using an integration interval of 2 seconds from launch to burnout.

Presented in figures 6(a) to 6(d) are plots of the aerodynamic-drag coefficients used in the calculations for the various configurations. The elements which made up these drag coefficients were based on wind-tunnel results from reference 9 and a compilation of empirical results from reference 10.

Values of C_{L_α} used for the four launch-package configurations were calculated from theory for configurations similar to those used in this paper. For configurations A, B, C, and D, the values of C_{L_α} used were, respectively, 0.0556 deg^{-1}, 0.0449 deg^{-1}, 0.0274 deg^{-1}, and 0.0375 deg^{-1}. These values were based on the total lifting-surface area (see table I) and were assumed constant throughout the Mach number range.

[redacted]

[redacted]

TRAJECTORIES AND STAGING

For the purposes of the calculations, it was assumed that each configuration was launched into a horizontal flight path with the simultaneous ignition of the first-stage booster engines and with an angle of attack of 15°. This angle of attack was held constant for a specified time, then a zero-g trajectory was induced and held until burnout. The time to change angle of attack was considered negligible. The time spent at an angle of attack of 15° was adjusted to obtain H
various flight-path angles at burnout of the last stage. The ideal 2
burnout point would be when the flight-path angle is zero and the alti- 2
tude and velocity are those required for equilibrium glide. 9

On the vehicles launched subsonically, the fins were dropped at the end of the pull-up. Fins were retained until the first-stage burnout on vehicles launched supersonically, since first-stage burnout occurred soon after the end of the pull-up.

At first-stage burnout, the first-stage boosters were immediately separated from the vehicle, and the second-stage booster ignited immediately and remained with the payload for the remainder of the trajectory. For the subsonically launched vehicles, staging occurred at dynamic pressures of 50 pounds per square foot, or less. For the supersonically launched vehicles, staging occurred at lower dynamic pressures.

Figures 7(a) and 7(b) show trajectories for typical subsonic and supersonic launches. Flight-path angle, velocity, dynamic pressure, altitude, and longitudinal acceleration are plotted against time.

RESULTS

Results of the various computations are presented in table II and in figure 8. The table shows the interpolated values at which a horizontal flight-path angle coincides with burnout, rather than the exact points of the computations. In actual flight, it would be necessary for burnout to occur when the vehicle altitude is near the equilibrium reentry path and also when the flight path is within 1° or 2° of horizontal. As can be seen in figures 8(a) to 8(h), these conditions are not always compatible. However, adjustments of the booster-thrust programing and the initial flight-path angle can often produce the desired results. Because of the preliminary nature of this investigation, only flight-path-angle variations were made. No attempt was made to adjust booster-thrust programing.

[redacted]

Orbital velocity is achieved when the relative velocity is about 24,600 feet per second, assuming an eastward launch from the latitudes of the southern part of the United States. The study showed that a 10,000-pound payload could reach this orbital velocity from the subsonic-launch condition by means of booster configurations B and C_2 (figs. 8(c) and 8(e)). However, vacuum specific-impulse values of about 335 seconds would be required. The supersonic-launch condition reduces the required vacuum specific impulse to 305 and 301 seconds for B and C_2 booster configurations, respectively (figs. 8(d) and 8(f)). It also permits the use of booster configuration D, but, again, a vacuum specific impulse of 335 seconds is required (fig. 8(h)). Thus, it is apparent that the advantange of the supersonic launch can be lost if it is necessary to use a high-drag configuration such as type D.

H
2
2
9

Although not as significant as orbital velocity, a velocity of 20,000 feet per second is a valuable research goal. A vehicle attaining speeds in this range can experience the maximum heating rates of a reentering orbital vehicle. Figure 8(b) shows that such a velocity can be attained with a single-stage 150,000-pound booster package, with a vacuum specific impulse of less than 340 seconds, launched subsonically. To avoid duplication of booster-development effort, a practical plan might be to construct a type C booster which initially will attain velocities in excess of 20,000 feet per second, but not orbital speed. Engine and structural improvements or, possibly, a switch to a supersonic launch would permit future attainment of orbital speeds.

The various booster configurations are compared on the basis of vacuum specific impulse and burnout velocity in figure 9(a) for the subsonic launch and in figure 9(b) for the supersonic launch. These data are combined in figure 10, which shows the incremental velocity resulting from deviations in vacuum specific impulse from a value of 320 seconds. A 1-percent increase in vacuum specific impulse results in about a 1-percent increase in burnout velocity; therefore, a 1-second change in vacuum specific impulse results in a change of about 70 feet per second in burnout velocity.

For a subsonic launch, burnout velocities of various payload weights with a type C booster are shown in figure 11. The effect on burnout velocity of variations in the ratio of payload weight to gross weight was investigated for the configuration C booster both by varying the payload weight with a constant gross weight and by varying the gross weight for a constant payload weight. The results are compatible, as shown in figure 12. Changing the payload weight by 1 percent of the launch-package gross weight from the nominal value of 5 percent affects the maximum velocity inversely by 1,400 feet per second for the type C booster launched subsonically.

[redacted]

For most of the computations, the structural weight was 4 percent of the combined fuel and structure weight. For the type A booster configuration, values of 2 percent and 4 percent were used; for the type C booster, values of 4 percent and 8 percent were used. The effect of the variations is shown in figure 13. Decreasing the ratio of structural weight to fuel-plus-structure weight from 4 percent to 3 percent increases the burnout velocity by 750 feet per second. Increasing this ratio from 4 percent to 5 percent will decrease the burnout velocity by 550 feet per second for the cases considered.

H229

CONCLUSIONS

From a preliminary performance analysis of the use of large bomber airplanes to air launch manned hypersonic and satellite vehicles, it is concluded that:

1. Booster packages weighing no more than 200,000 pounds are capable of accelerating a 10,000-pound winged vehicle to orbital velocity after being launched eastward from a subsonic bomber, if a vacuum specific impulse of about 335 seconds can be achieved in the booster engines.

2. For most of the booster configurations studied, a deviation of 1 percent in vacuum specific impulse from a nominal value of 320 seconds results in about a 1-percent variation in burnout velocity.

3. Increasing the ratio of payload weight to launch-package gross weight to 6 percent from a nominal value of 5 percent decreases the burnout velocity by 1,400 feet per second for the type C booster launched subsonically.

4. Configuration requirements imposed on the booster package by the launch airplane are an important consideration. In this study the high drag of the booster package required to fit the supersonic-launch airplane offsets the performance advantages of launching supersonically rather than subsonically.

Flight Research Center,
National Aeronautics and Space Administration,
Edwards, Calif., October 9, 1961.

[redacted]

[redacted]

REFERENCES

1. Ross, Malcolm D.: Aircraft Launched Rockets, Part I. Rockair. Sounding Rockets, Homer E. Newell, Jr., ed., McGraw-Hill Book Co., Inc., 1959, pp. 165-180.

2. Kraff, Louis, Jr., and Slavin, Robert M.: Aircraft Launched Rockets, Part II. Rockaire. Sounding Rockets, Homer E. Newell, Jr., ed., McGraw-Hill Book Co., Inc., 1959, pp. 181-189.

3. Robotti, Aurelio C.: Satellite Launching From an F-102. Missiles and Rockets, vol. 1, no. 2, Nov. 1956, pp. 54, 56, 58.

H229

4. Anon.: Navy's Air-Launch Satellite Program Starts Flight Tests Under "Caleb" Project at Mugu. Western Aviation, Missile and Space Industries, vol. 40, no. 10, Oct. 1960, pp. 4-5.

5. Kappus, Peter G.: Air-Breathing Power Plants in the Space Era. Aero/Space Eng., vol. 17, no. 11, Nov. 1958, pp. 62-65, 69.

6. Ferri, A., Daskim, W., Feldman, L., and Nucci, L. M.: The Launching of Space Vehicles by Air-Breathing Lifting Stages. Vol. 2 of Vistas in Astronautics. Part IV, Morton Alperin and Hollingsworth F. Gregory, eds., Pergamon Press, 1959, pp. 163-173.

7. Bulban, Erwin J.: B-52 Use as First-Stage Booster Studied. Aviation Week and Space Technology, vol. 75, no. 9, Aug. 28, 1961, pp. 72, 77.

8. Minzner, R. A., and Ripley, W. S.: The ARDC Model Atmosphere, 1956. Air Force Surveys in Geophysics No. 86 (AFCRC-TN-56-204), Air Force Cambridge Res. Center (Bedford, Mass.), Dec. 1956.

9. Johnston, Patrick J., and Ladson, Charles L.: Experimental Investigation of Longitudinal Static Stability of a Glider and 11 Booster Configurations at Mach Numbers From 1.62 to 6.86. NASA TM X-356, 1961.

10. Hoerner, Sighard F.: Fluid-Dynamic Drag. Pub. by the author (148 Busteed Dr., Midland Park, N. J.), 1958.

[redacted]

[redacted]

TABLE I.- PHYSICAL CHARACTERISTICS OF THE BOOSTER CONFIGURATIONS

Configuration	Launch weight, lb	Overall length, ft	Booster diameter, ft	Total horizontal-lifting area, sq ft	Payload weight, lb	Number of stages	Number of engines		Thrust, per engine, lb	Fuel weight, lb		Structure weight, lb	Structure, percent of fuel	Engine weight, per engine, lb	Fin area	
							First stage	Second stage		First stage	Second stage				Horizontal, sq ft	Vertical, sq ft
A_1	150,000	75.0	10	900	10,000	1	3	------	100,000	129,380	------	2,640	2.04	1,250	425	280
A_2	150,000	75.0	10	900	10,000	1	3	------	100,000	126,720	------	5,280	4.16	1,250	425	280
B	200,000	98.0	8	688	10,000	2	2	1	150,000	122,525	51,575	7,260	4.16	1,900	290	200
C_1	200,000	64.5	7	1,020	5,000	2	2	1	150,000	135,468	42,600	7,420	4.16	1,900	392	260
C_2	200,000	64.5	7	1,020	10,000	2	2	1	150,000	119,796	53,472	7,220	4.16	1,900	392	260
C_3	200,000	64.5	7	1,020	15,000	2	2	1	150,000	107,388	61,080	7,020	4.16	1,900	392	260
C_4	200,000	64.5	7	1,020	10,000	2	2	1	150,000	123,200	42,849	14,439	8.70	1,900	392	260
C_5	190,000	64.5	7	1,020	10,000	2	2	1	150,000	114,943	41,906	13,639	8.70	1,900	392	260
C_6	180,000	64.5	7	1,020	10,000	2	2	1	150,000	106,709	40,940	12,839	8.70	1,900	392	260
C_7	160,000	64.5	7	1,020	10,000	2	2	1	150,000	90,264	38,985	11,239	8.70	1,900	392	260
D	200,000	39.3	6	690	10,000	2	2	1	150,000	119,796	53,472	7,220	4.16	1,900	392	260

[redacted]

[redacted]

TABLE II.- RESULTS OF THE COMPUTATIONS FOR A FLIGHT-PATH ANGLE OF ZERO AT BURNOUT

Configuration	I_{sp}, sec	Thrust, lb		Launch conditions		Burnout conditions		Total burning time, sec
		First stage	Second stage	h, ft	M	h, ft	V, ft/sec	
A_1	300	300,000	------------	35,000	0.7	131,000	19,185	129.38
	320		------------			144,000	20,460	138.01
	340		------------			149,000	21,800	146.63
A_2	300		------------	35,000	0.7	122,000	17,830	126.72
	320		------------			134,000	19,050	135.17
	340		------------			139,500	20,200	143.62
B	300		150,000	35,000	0.7	250,000	21,700	225.68
	320					270,000	23,230	240.69
	340					290,000	24,680	255.34
	300			75,000	3.0	288,000	24,240	225.68
	320					302,000	25,760	240.69
	340					313,000	27,290	255.34
C_1	300			35,000	0.7	218,000	26,420	220.67
	320					235,000	28,150	235.38
	340					247,000	30,100	250.09
C_2	300			35,000	0.7	254,000	21,990	226.74
	320					275,000	23,500	241.85
	340					294,000	25,030	256.97
	300			75,000	3.0	291,000	24,550	226.74
	320					305,000	26,150	241.85
	340					315,000	27,700	256.97
C_3	300			35,000	0.7	280,000	18,950	229.55
	320					305,000	20,250	244.85
	340					331,000	21,580	260.16
C_4	320			35,000	0.7	247,500	21,750	222.72
C_5	320			35,000	0.7	232,500	21,440	212.01
C_6	320			35,000	0.7	218,000	21,050	201.16
C_7	320			35,000	0.7	192,000	20,170	179.45
D	300			35,000	0.7	216,000	19,720	226.74
	320					233,000	21,270	241.85
	340					255,000	22,810	256.97
	300			75,000	3.0	255,000	22,000	226.74
	320					268,000	23,460	241.85
	340					281,000	24,940	256.97

[redacted]

[redacted]

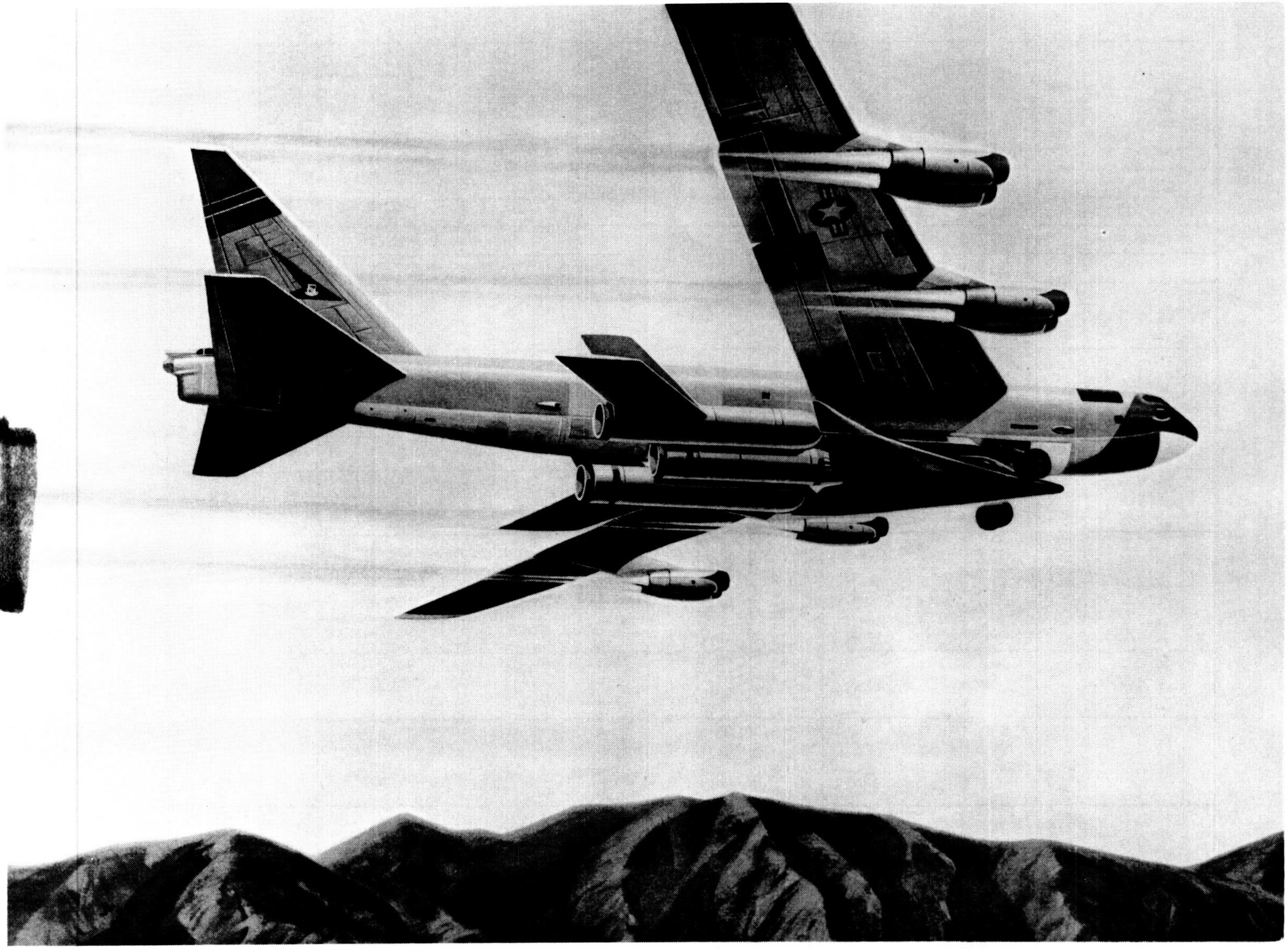

Figure 1.- Artist's conception of a subsonic airplane carrying one of the booster-payload configurations.

E-6862

[redacted]

H-229

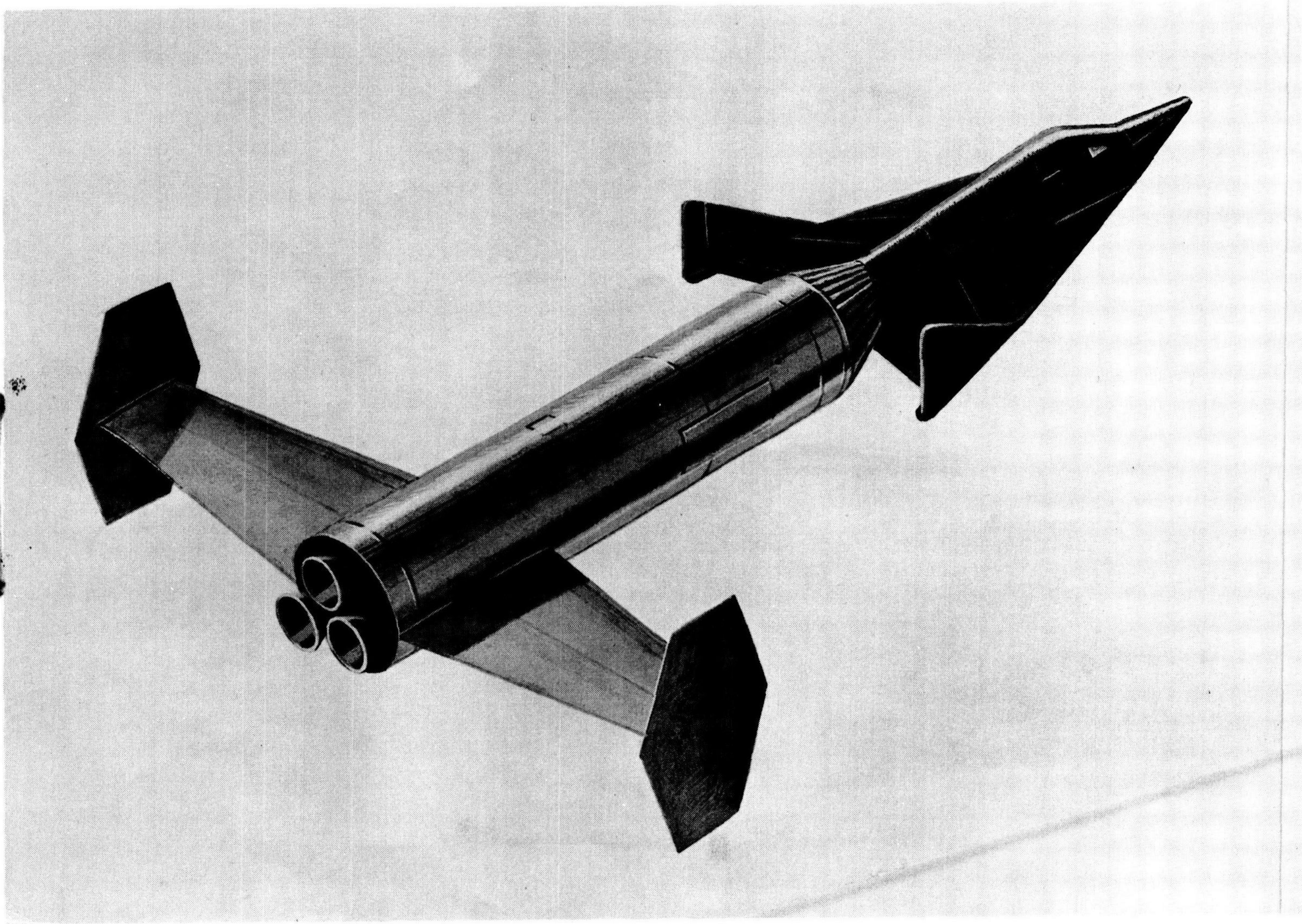

Figure 2.- Drawing of payload and type A booster.

[redacted]

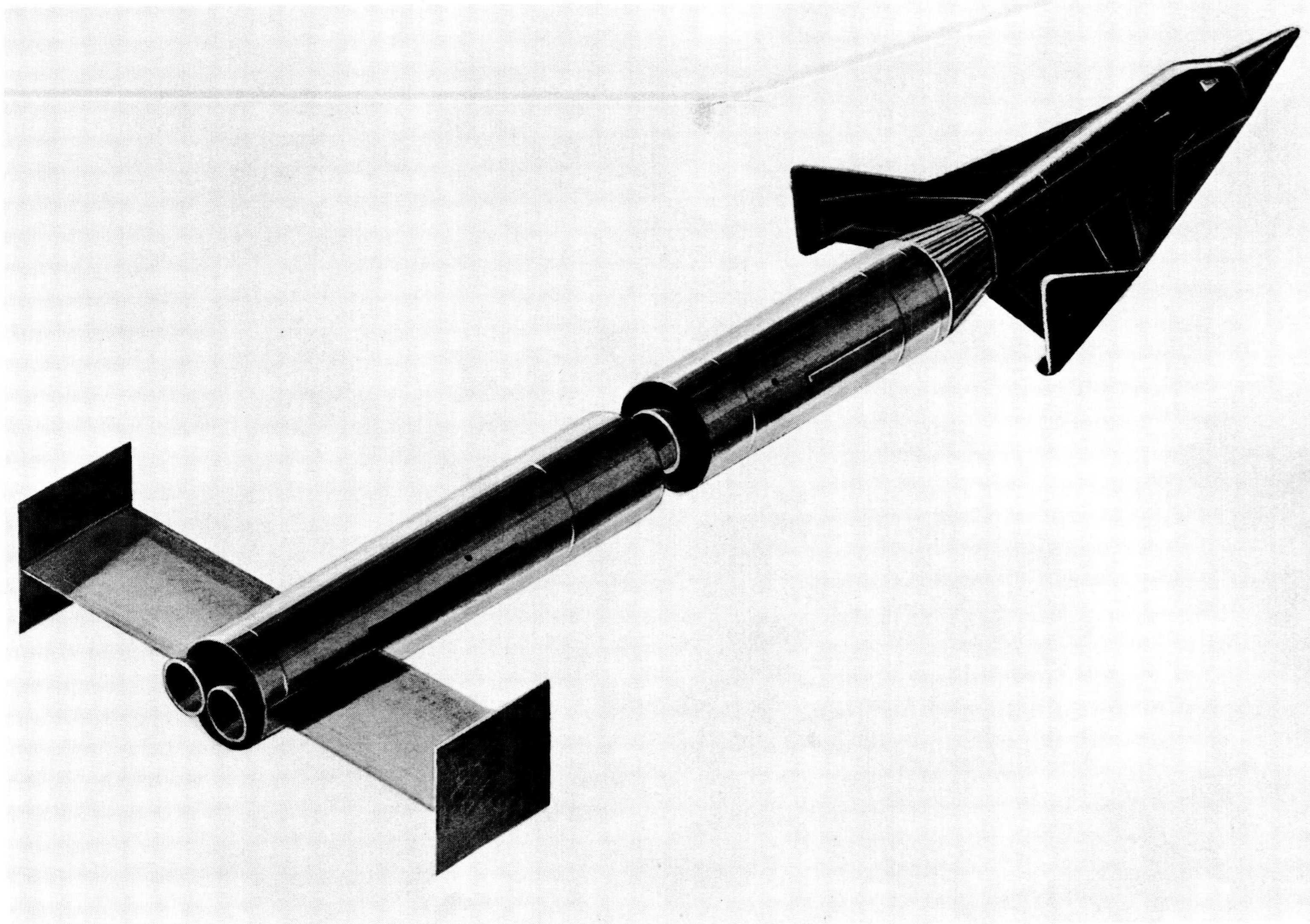

Figure 3.- Drawing of payload and type B booster.

[redacted]

[redacted]

H-229

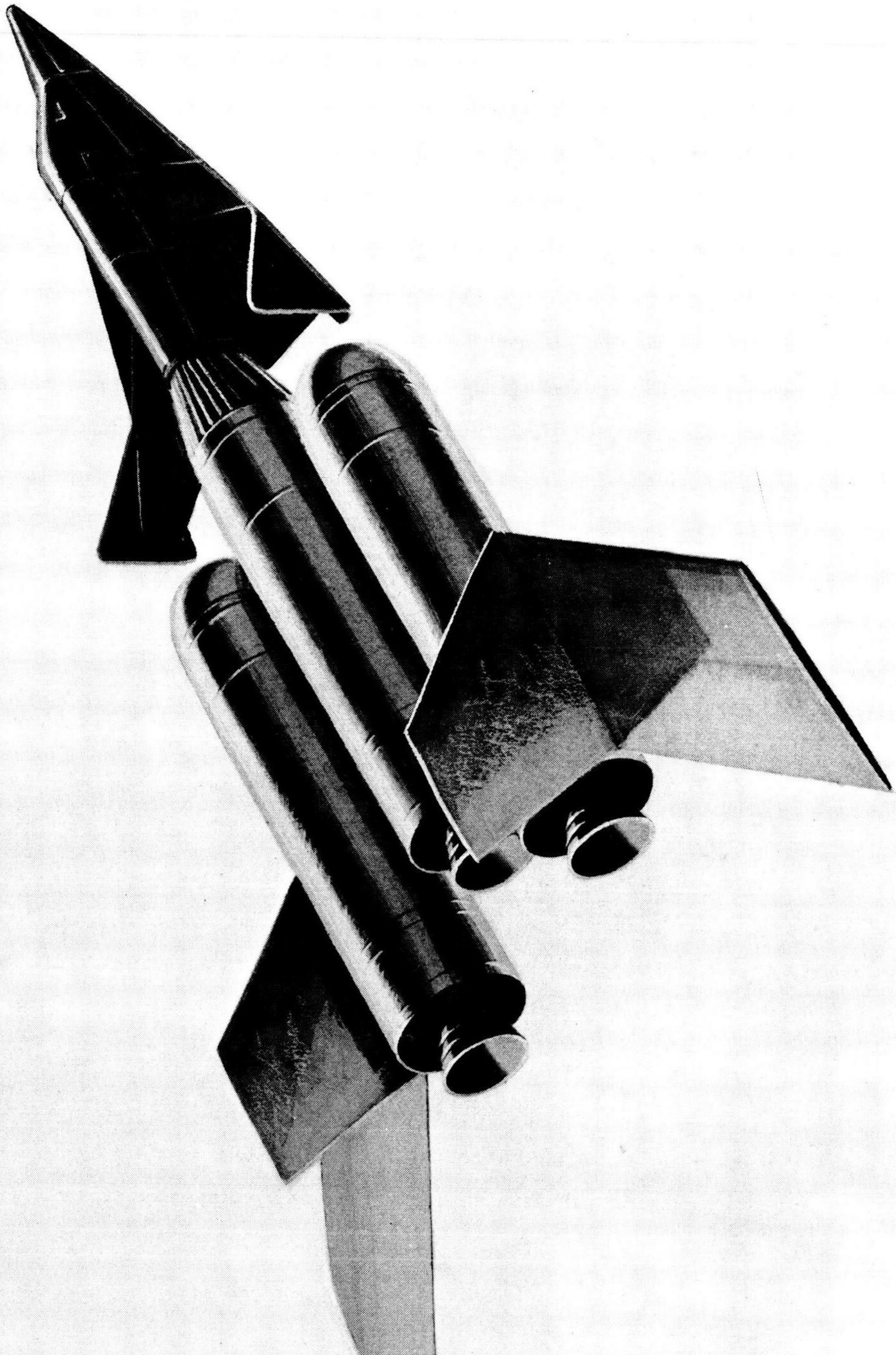

Figure 4.- Drawing of payload and type C booster.

[redacted]

[redacted]

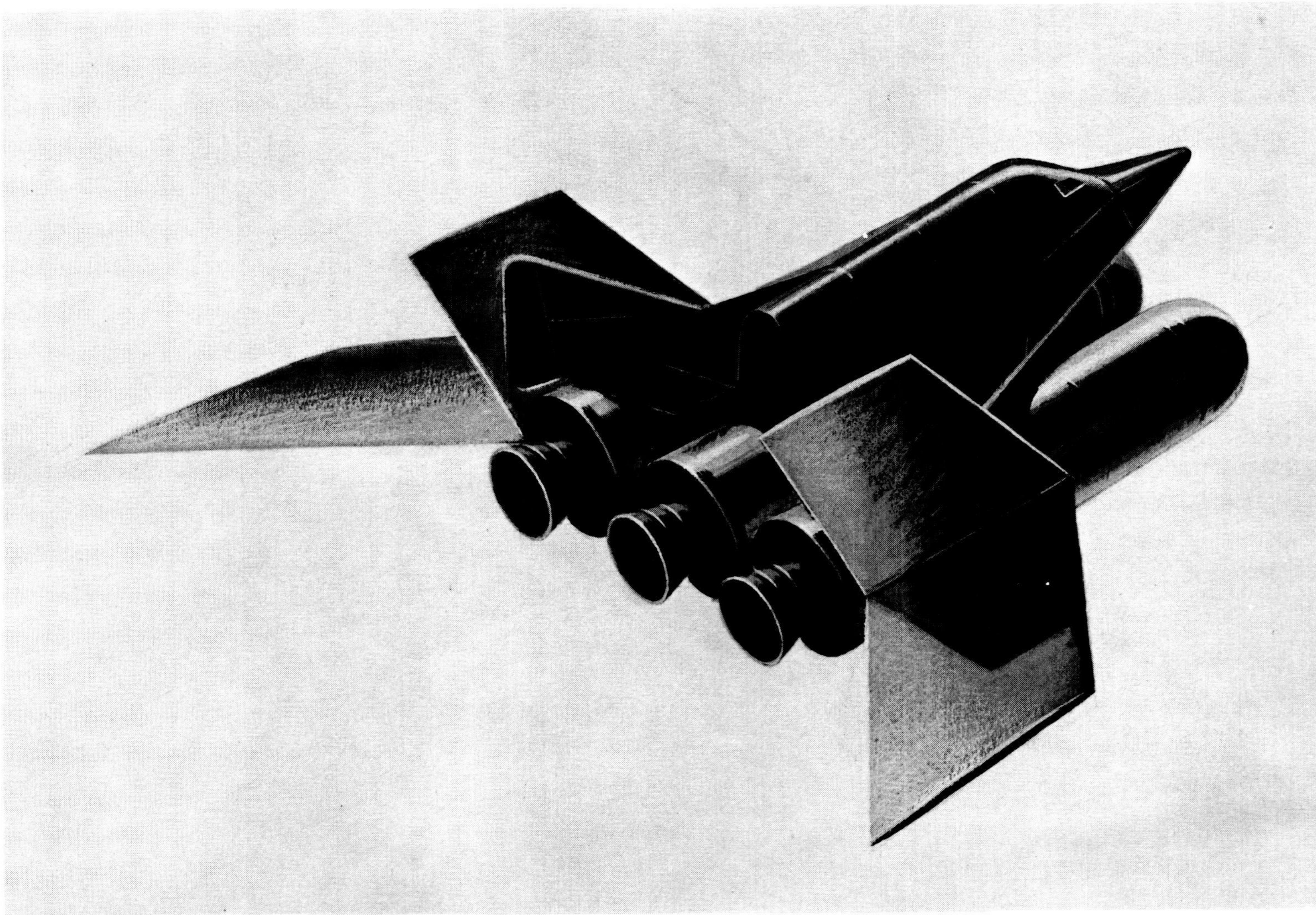

Figure 5.- Drawing of payload and type D booster.

[redacted]

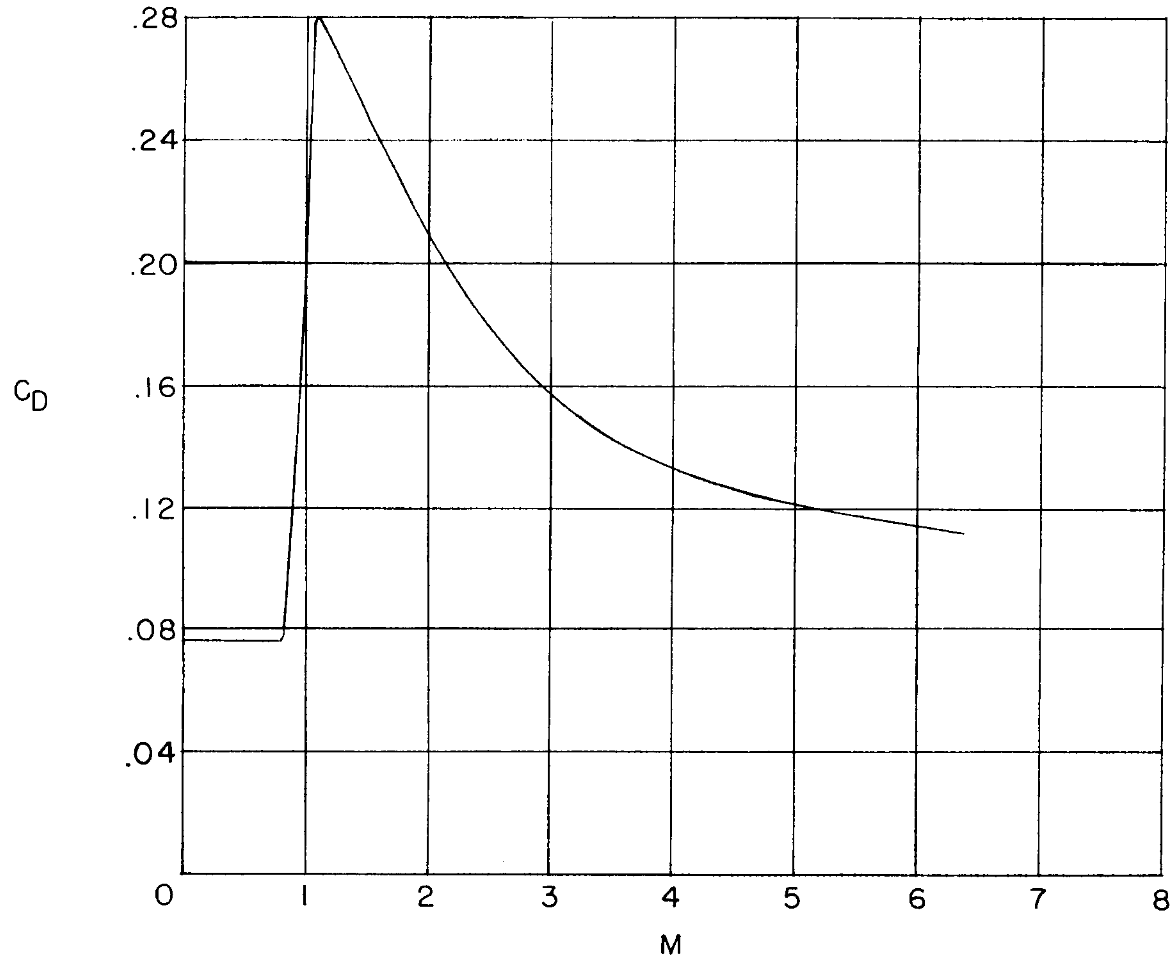

(a) Type A booster-payload configuration.

Figure 6.- Aerodynamic zero-lift drag characteristics used in the calculations. Reference area = 330 square feet.

[redacted]

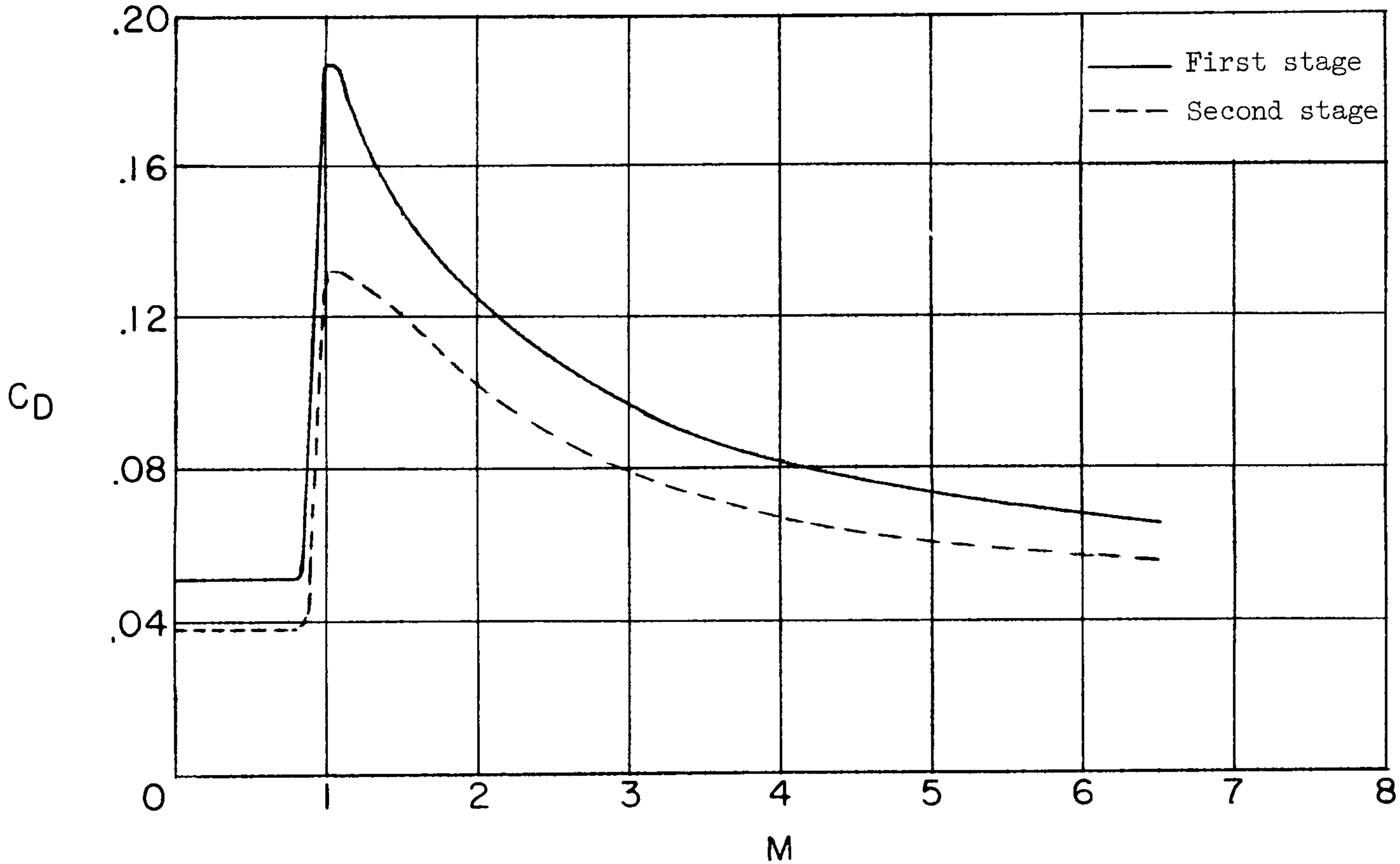

(b) Type B booster-payload configuration.

Figure 6.- Continued.

[redacted]

[redacted]

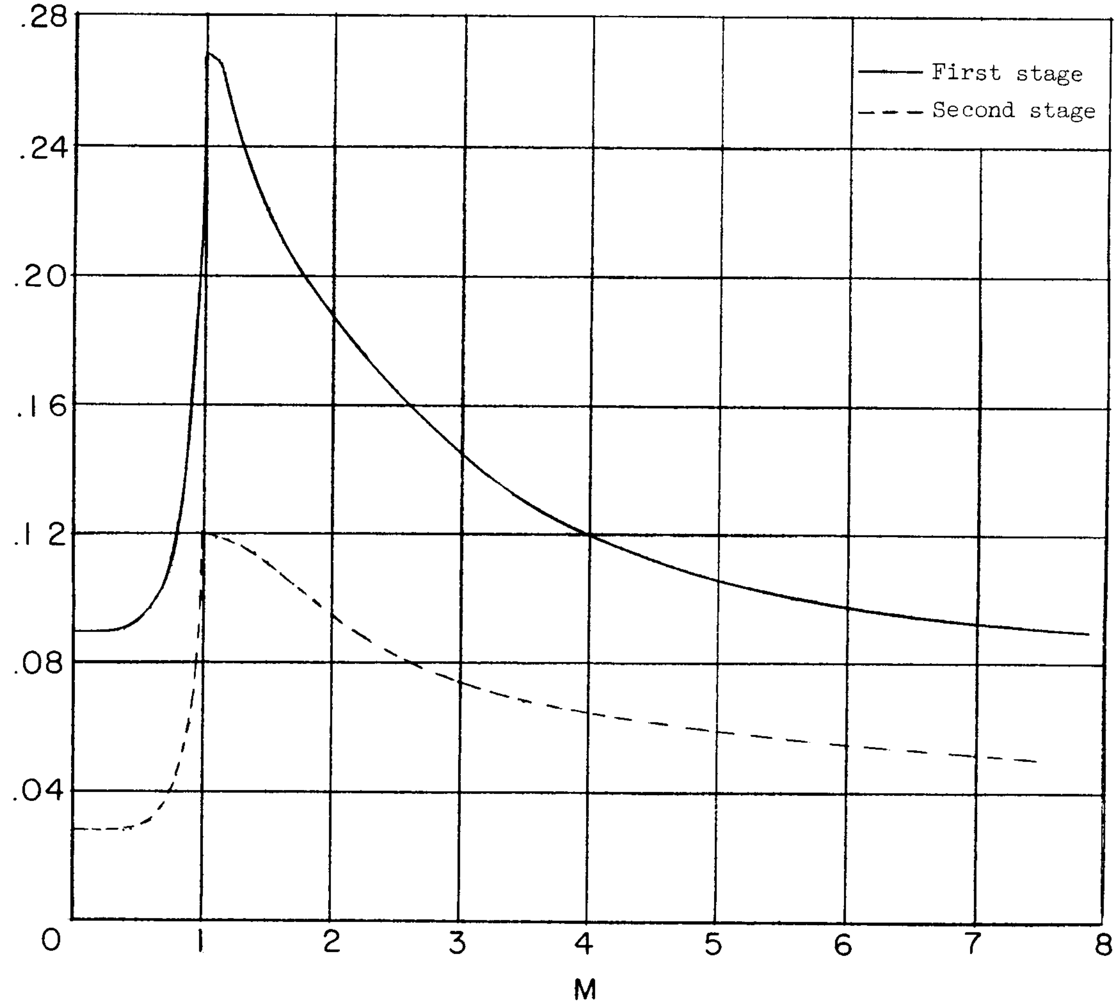

(c) Type C booster-payload configuration.

Figure 6.- Continued.

[redacted]

[redacted]

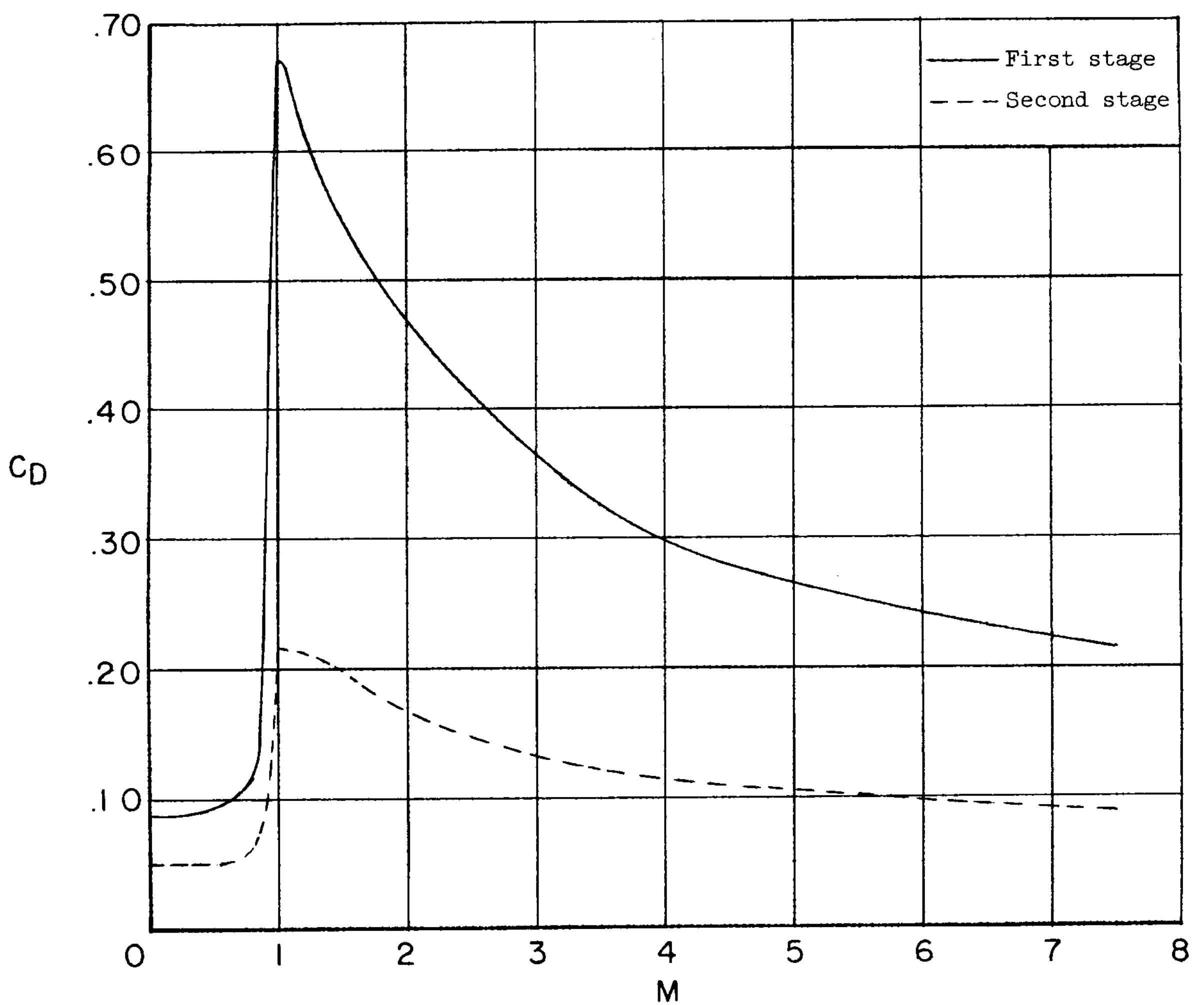

(d) Type D booster-payload configuration.

Figure 6.- Concluded.

[redacted]

[redacted]

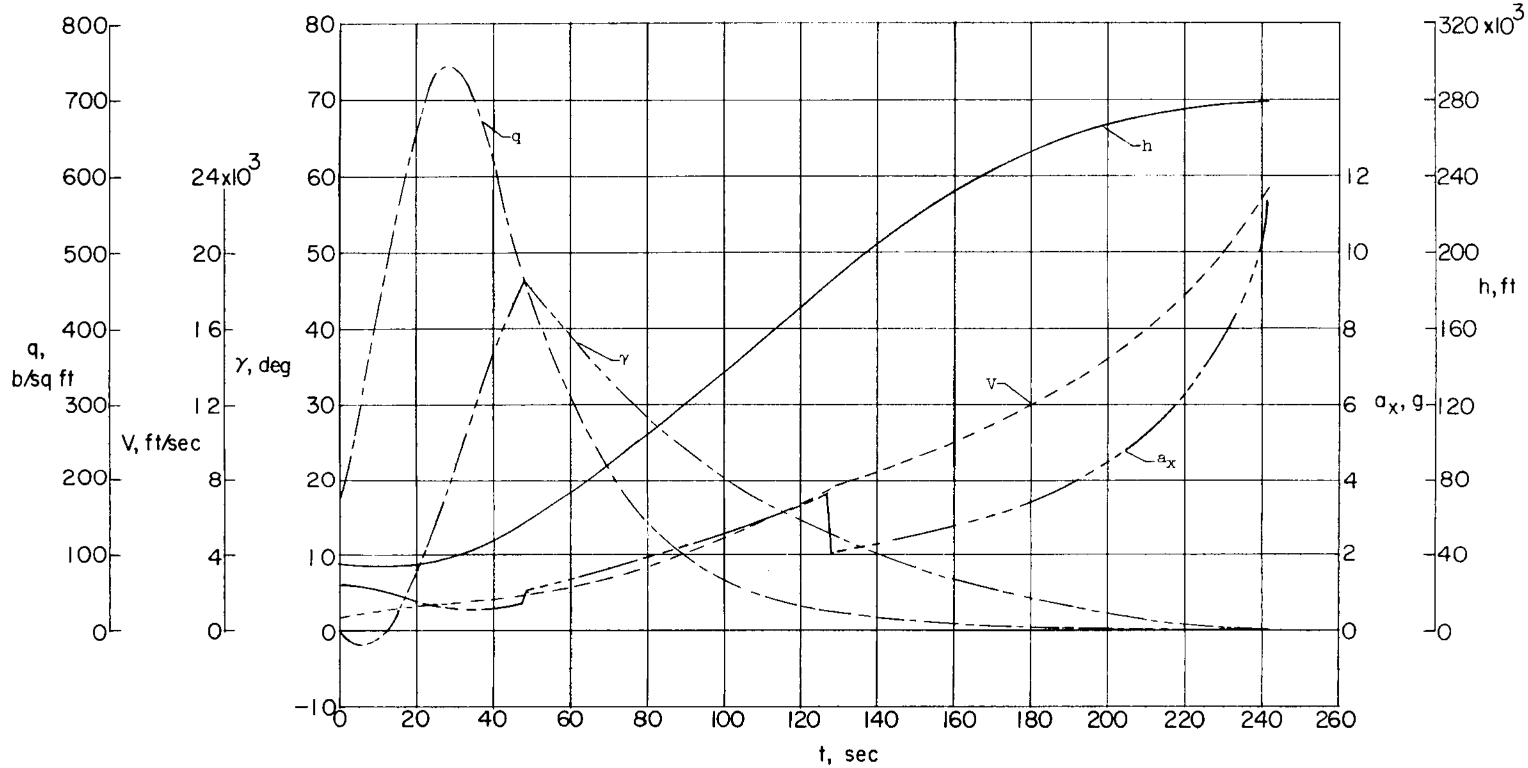

(a) Subsonic launch.

Figure 7.- Typical time histories of altitude, velocity, flight-path angle, and dynamic pressure from launch to burnout.

[redacted]

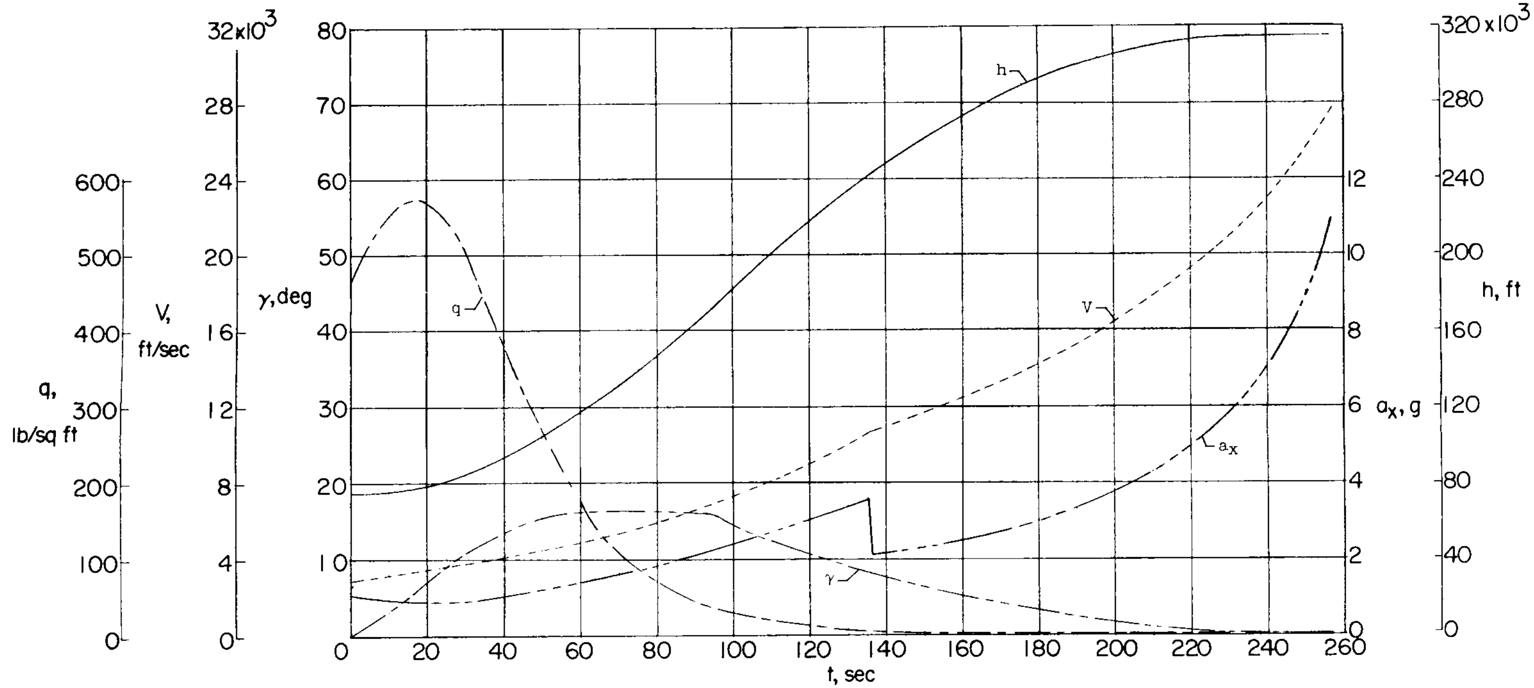

(b) Supersonic launch.

Figure 7.- Concluded.

[redacted]

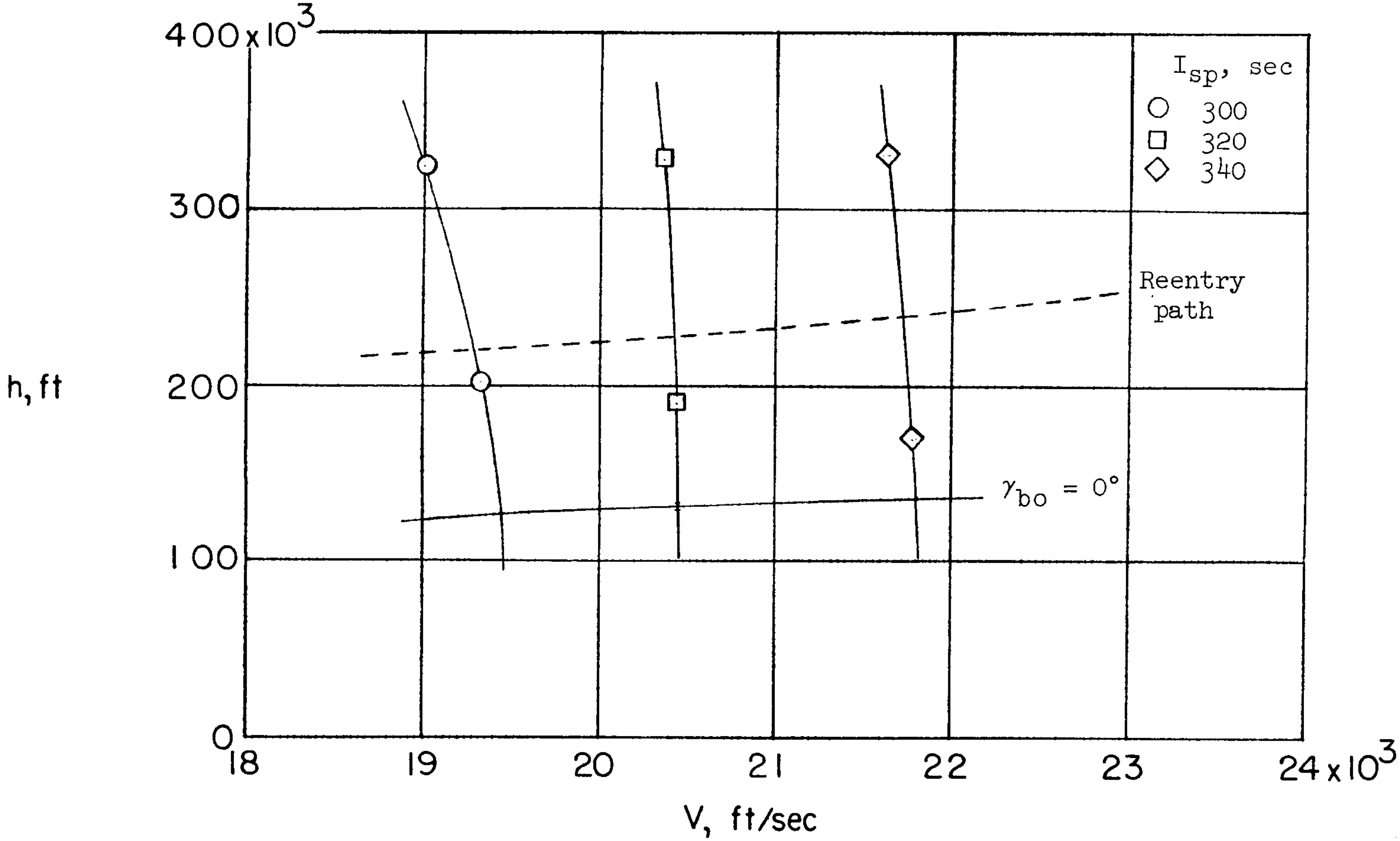

(a) Configuration A_1, subsonic launch.

Figure 8.- Loci of burnout velocities for different values of specific impulse.

[redacted]

[redacted]

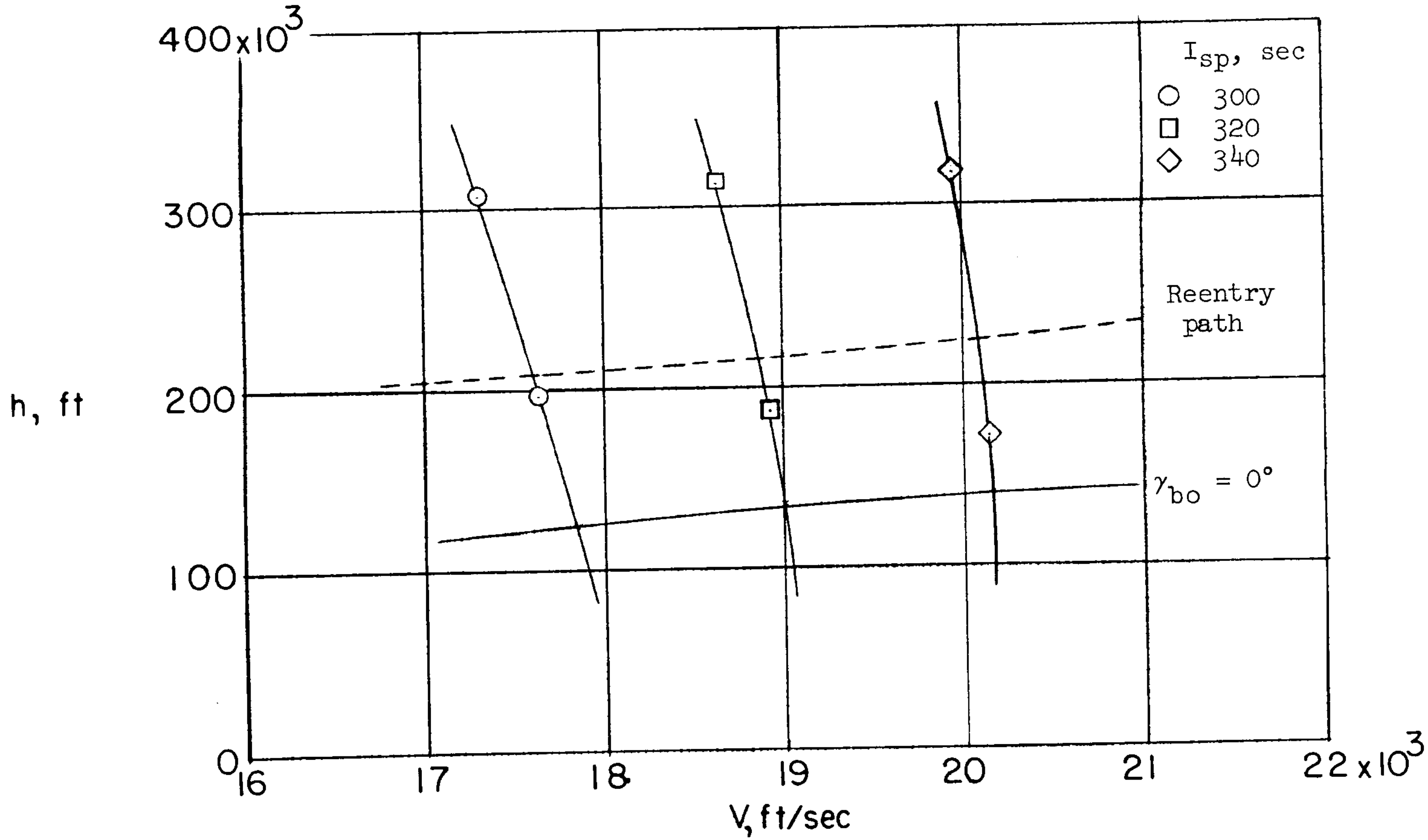

(b) Configuration A_2, subsonic launch.

Figure 8.- Continued.

[redacted]

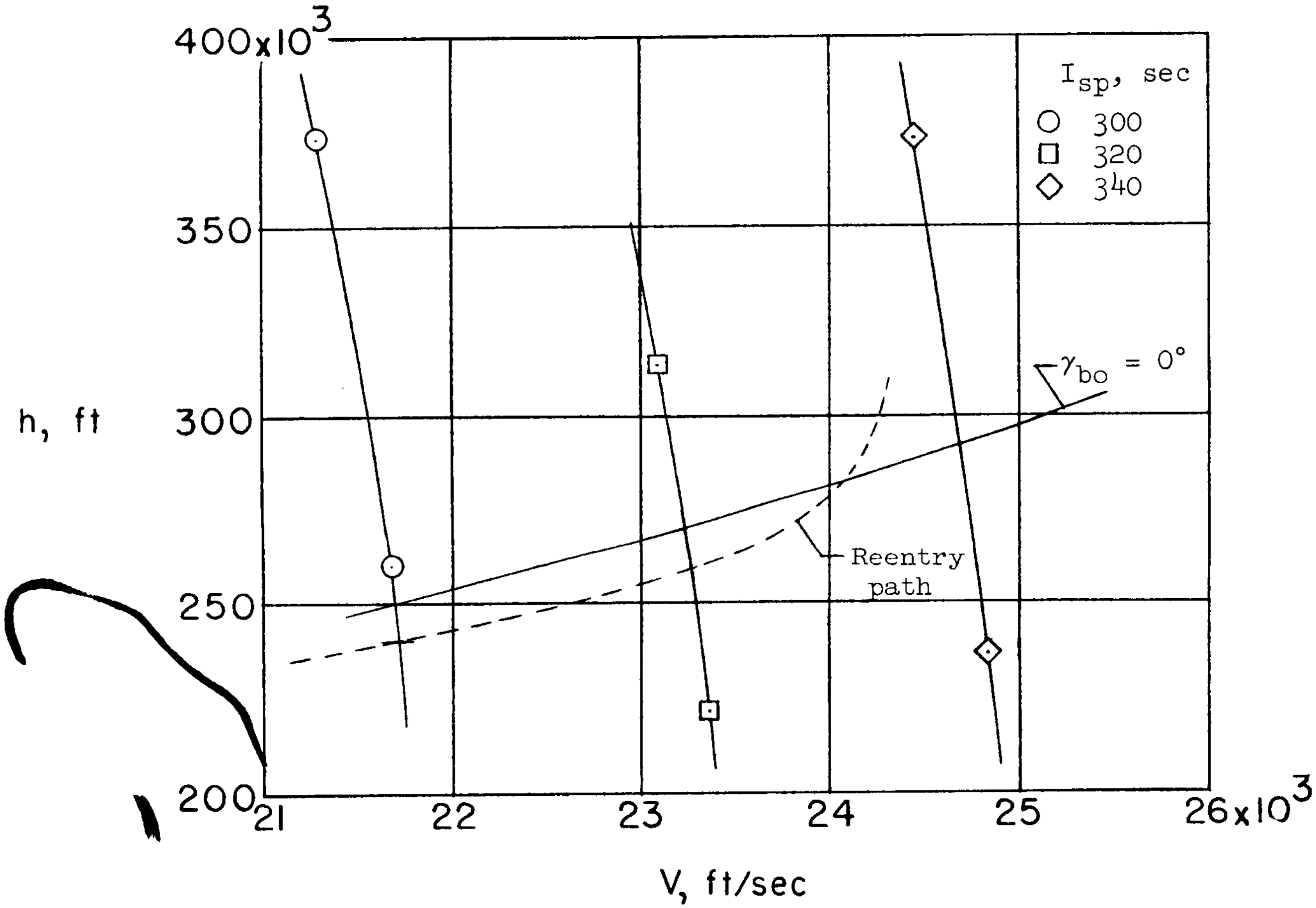

(c) Configuration B, subsonic launch.

Figure 8.- Continued.

[redacted]

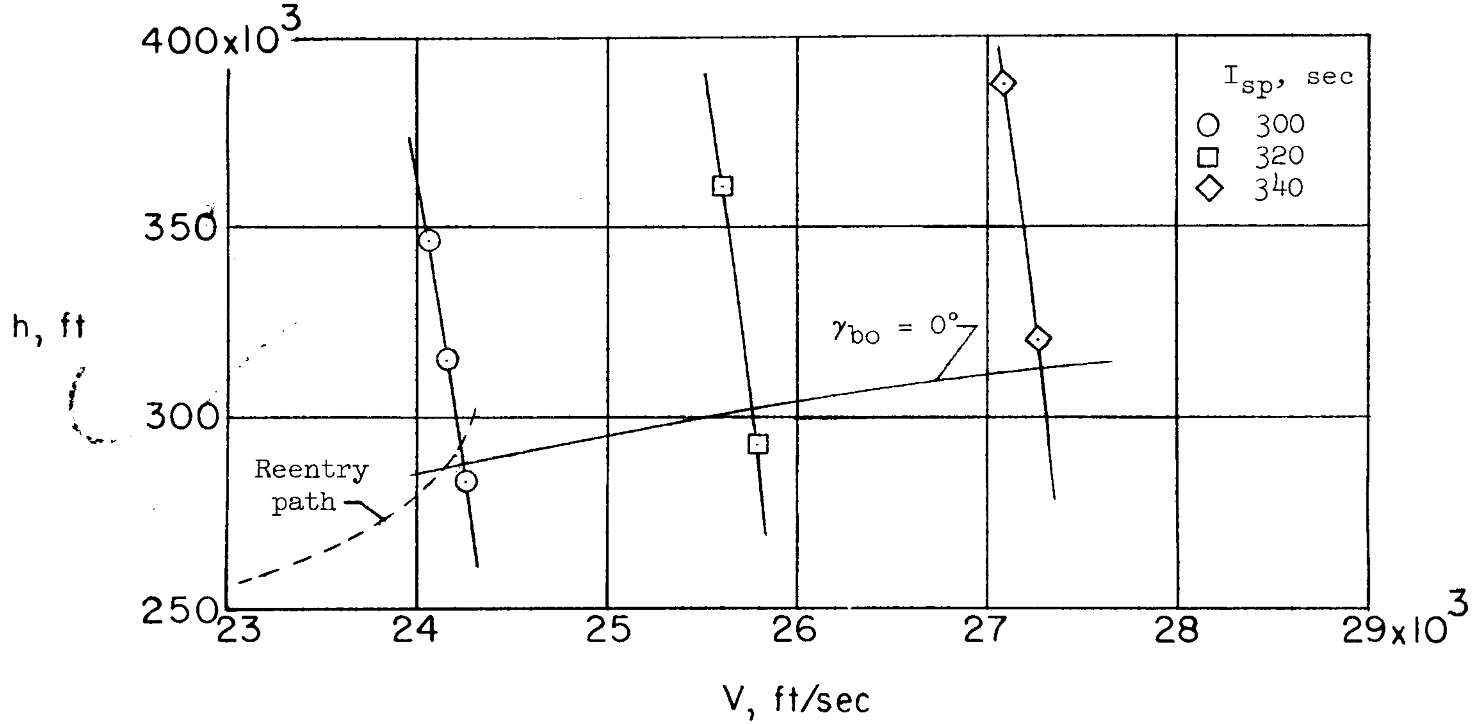

(d) Configuration B, supersonic launch.

Figure 8.- Continued.

[redacted]

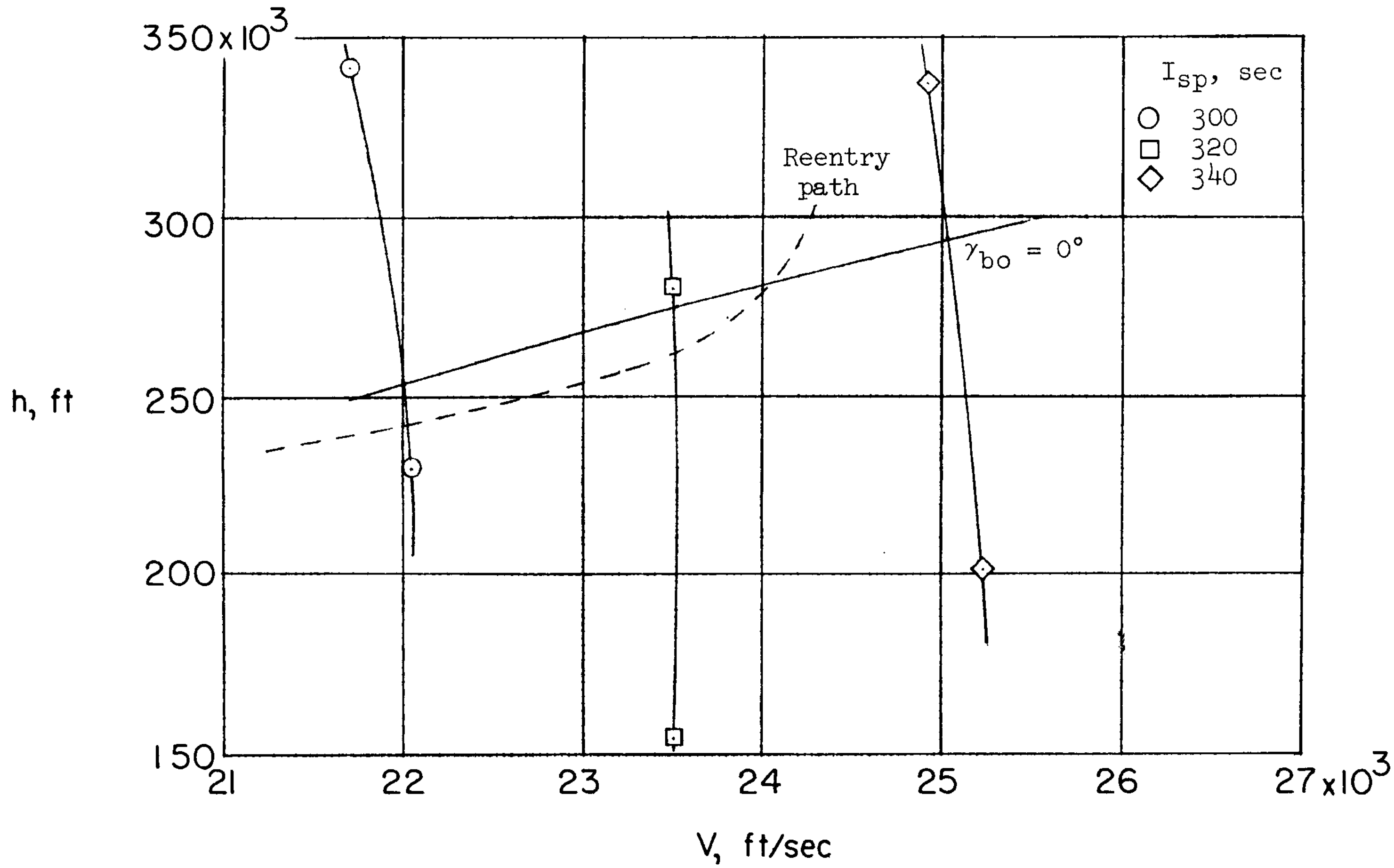

(e) Configuration C_2, subsonic launch.

Figure 8.- Continued.

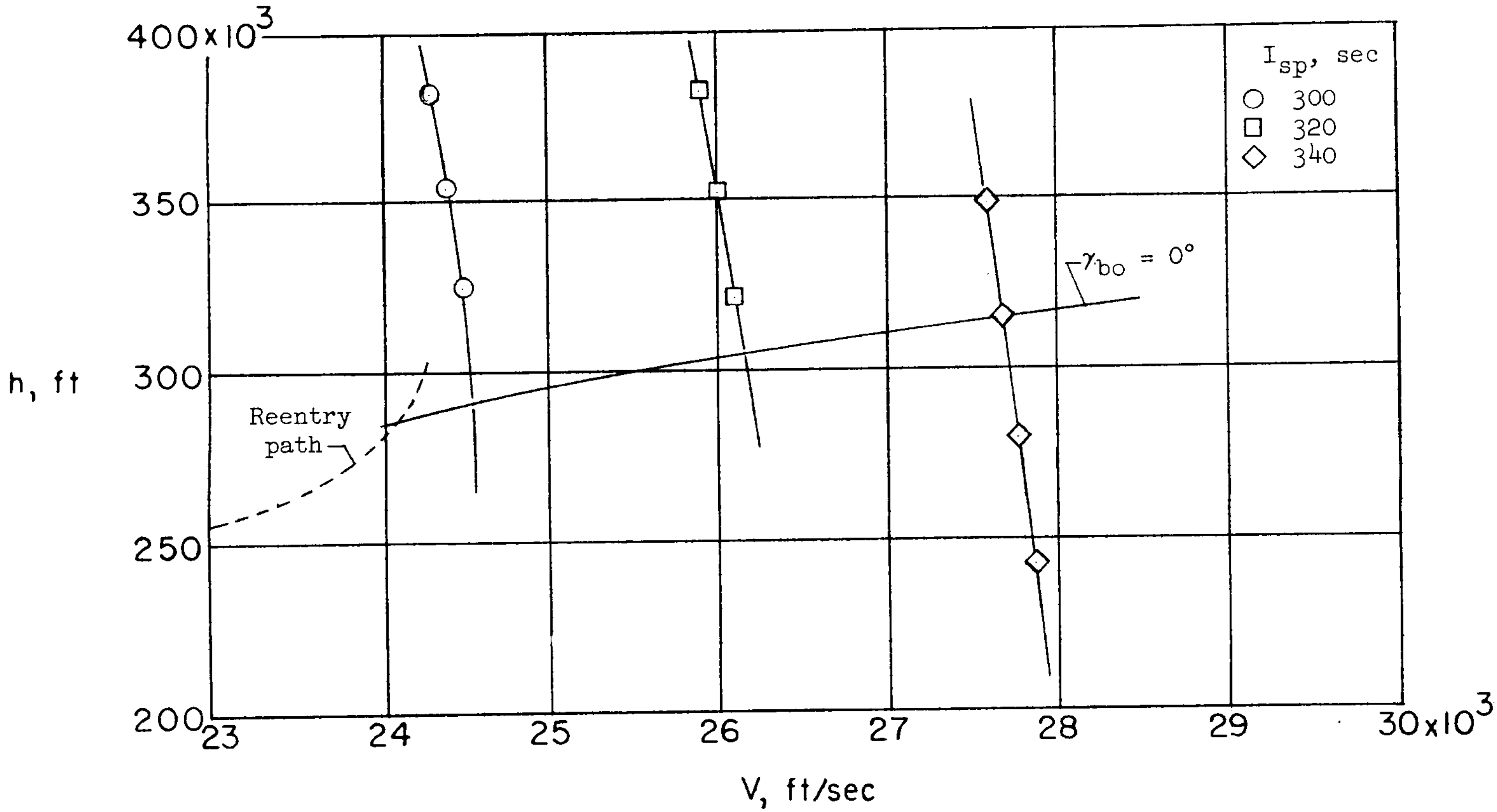

(f) Configuration C_2, supersonic launch.

Figure 8.- Continued.

[redacted]

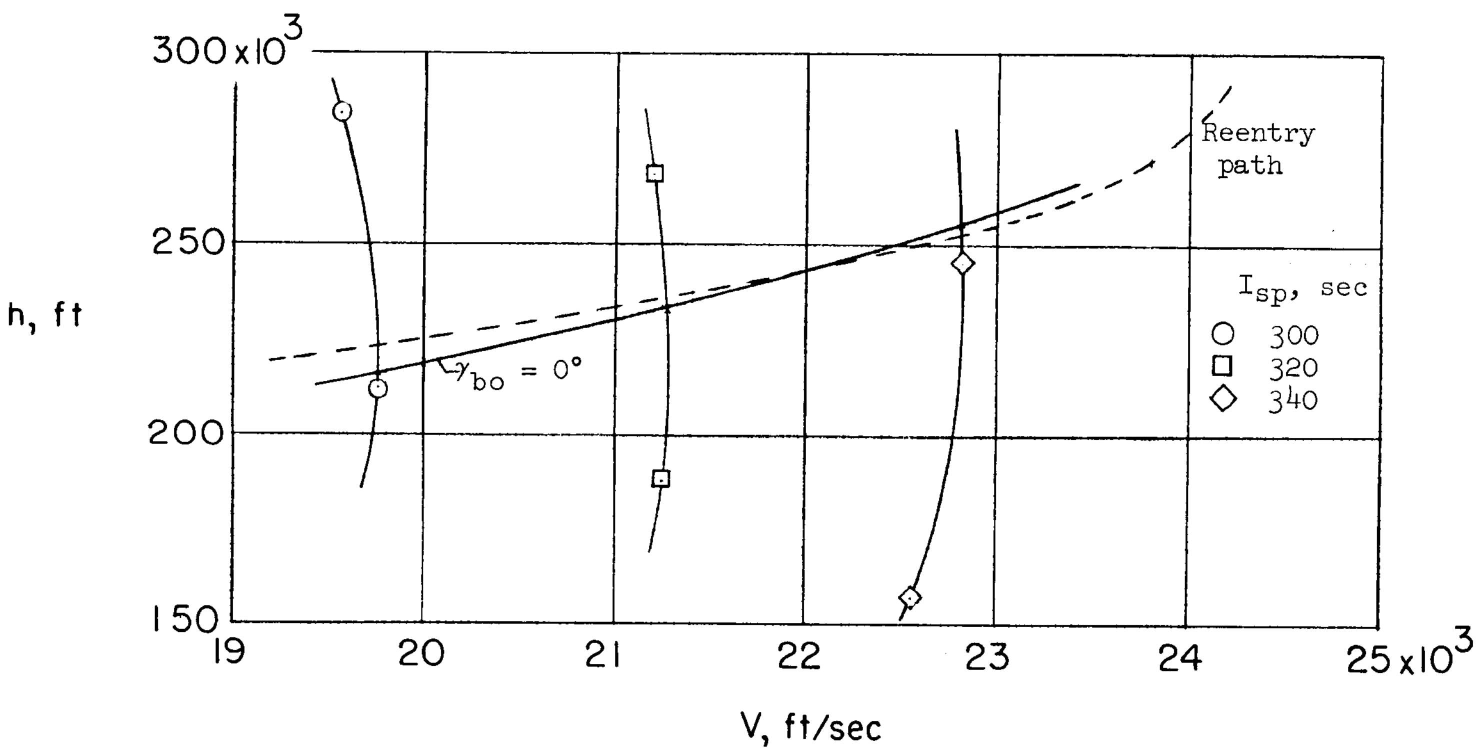

(g) Configuration D, subsonic launch.

Figure 8.- Continued.

[redacted]

[redacted]

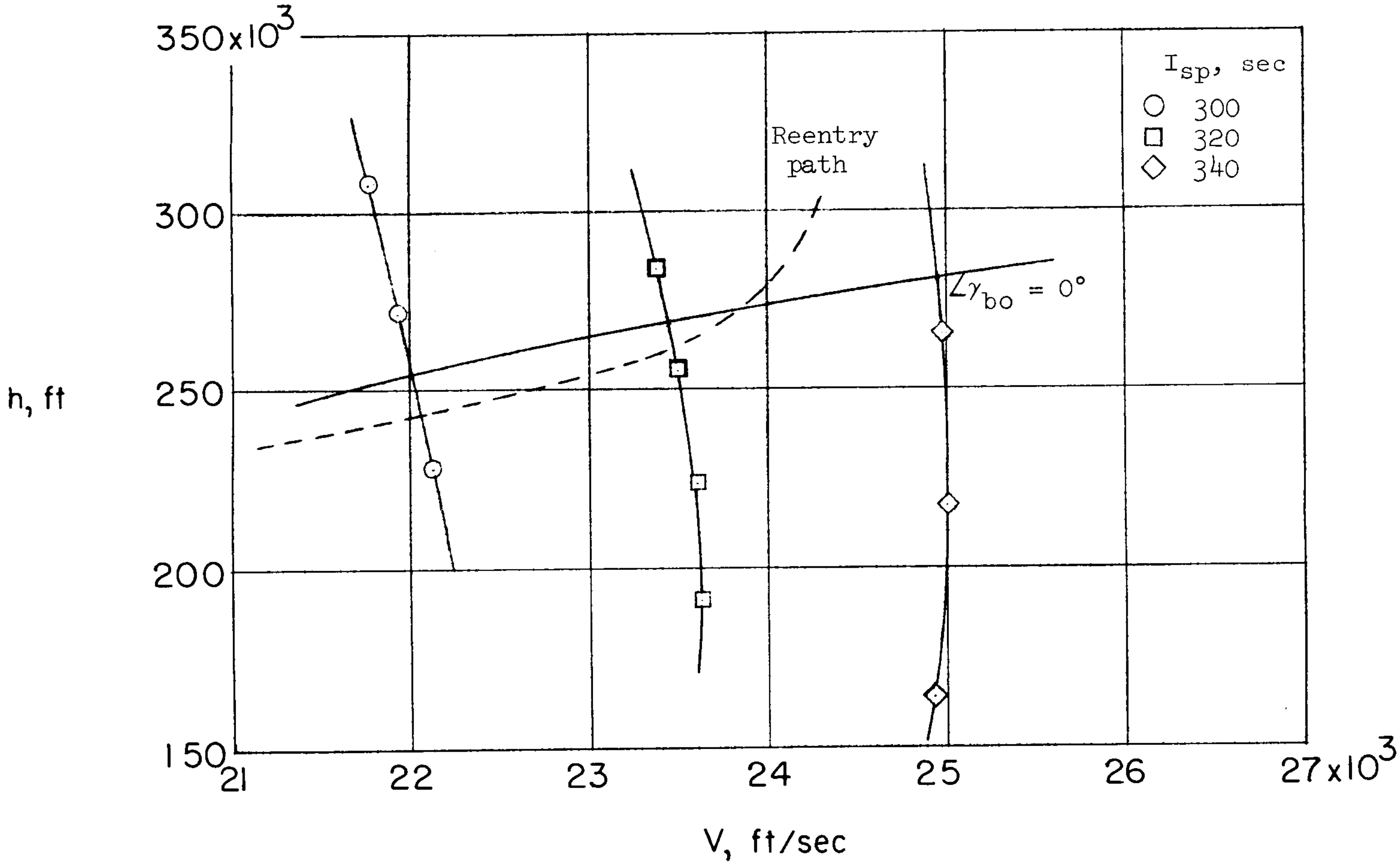

(h) Configuration D, supersonic launch.

Figure 8.- Concluded.

[redacted]

[redacted]

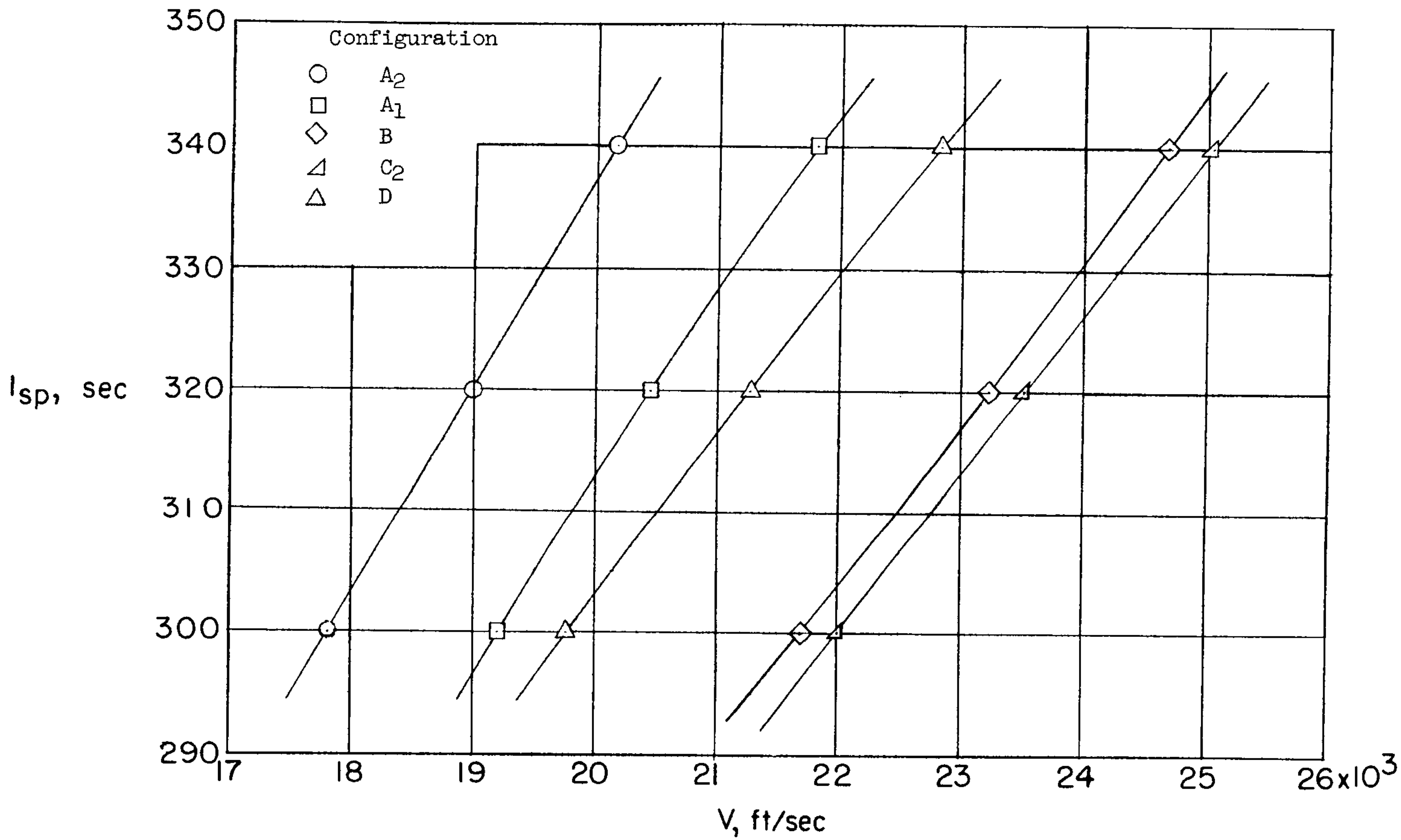

(a) Subsonic launches.

Figure 9.- Comparison of booster-vehicle configurations on the basis of vacuum specific impulse and burnout velocity. $\gamma_{bo} = 0°$.

[redacted]

[redacted]

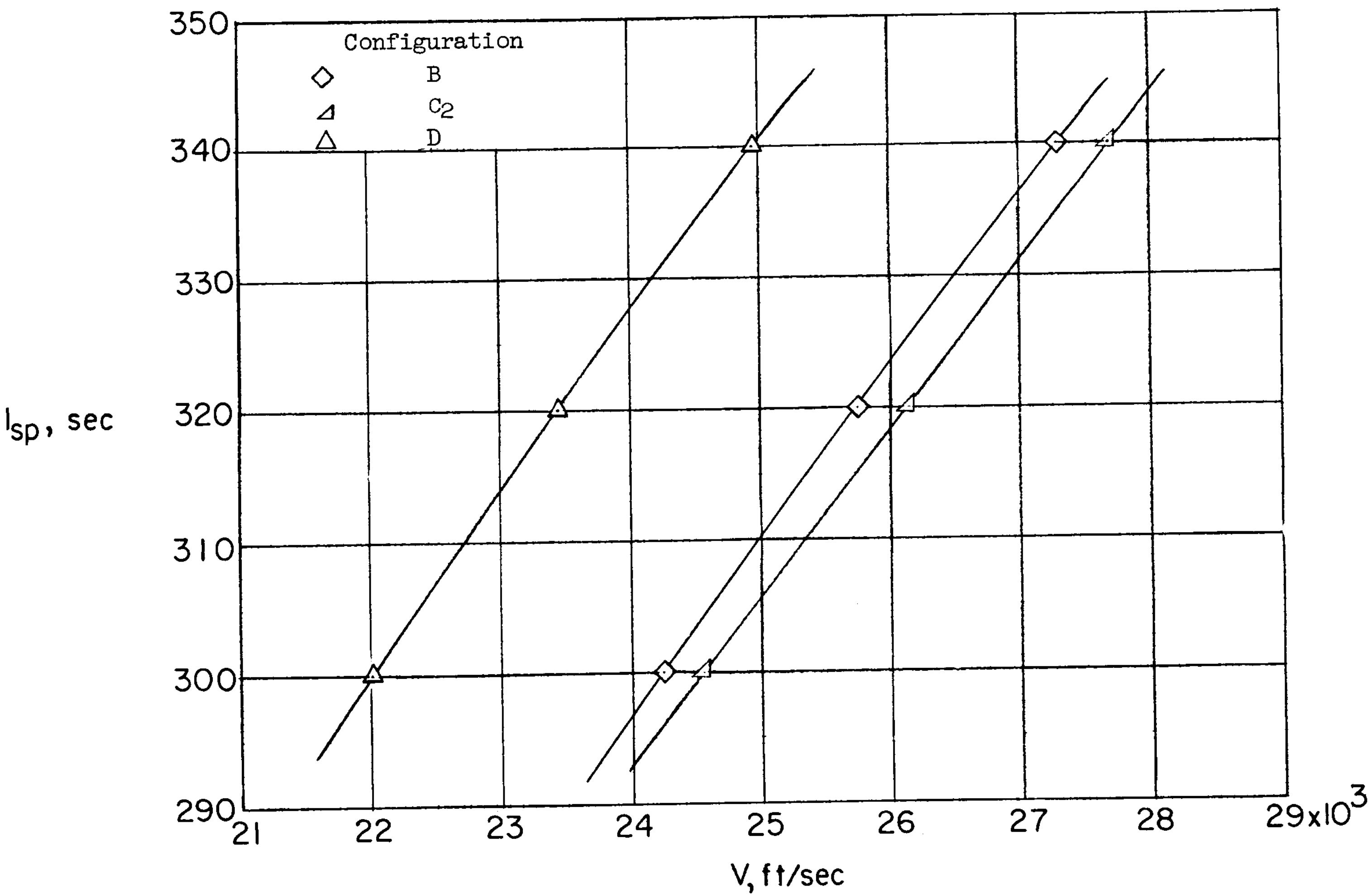

(b) Supersonic launches.

Figure 9.- Concluded.

[redacted]

[redacted]

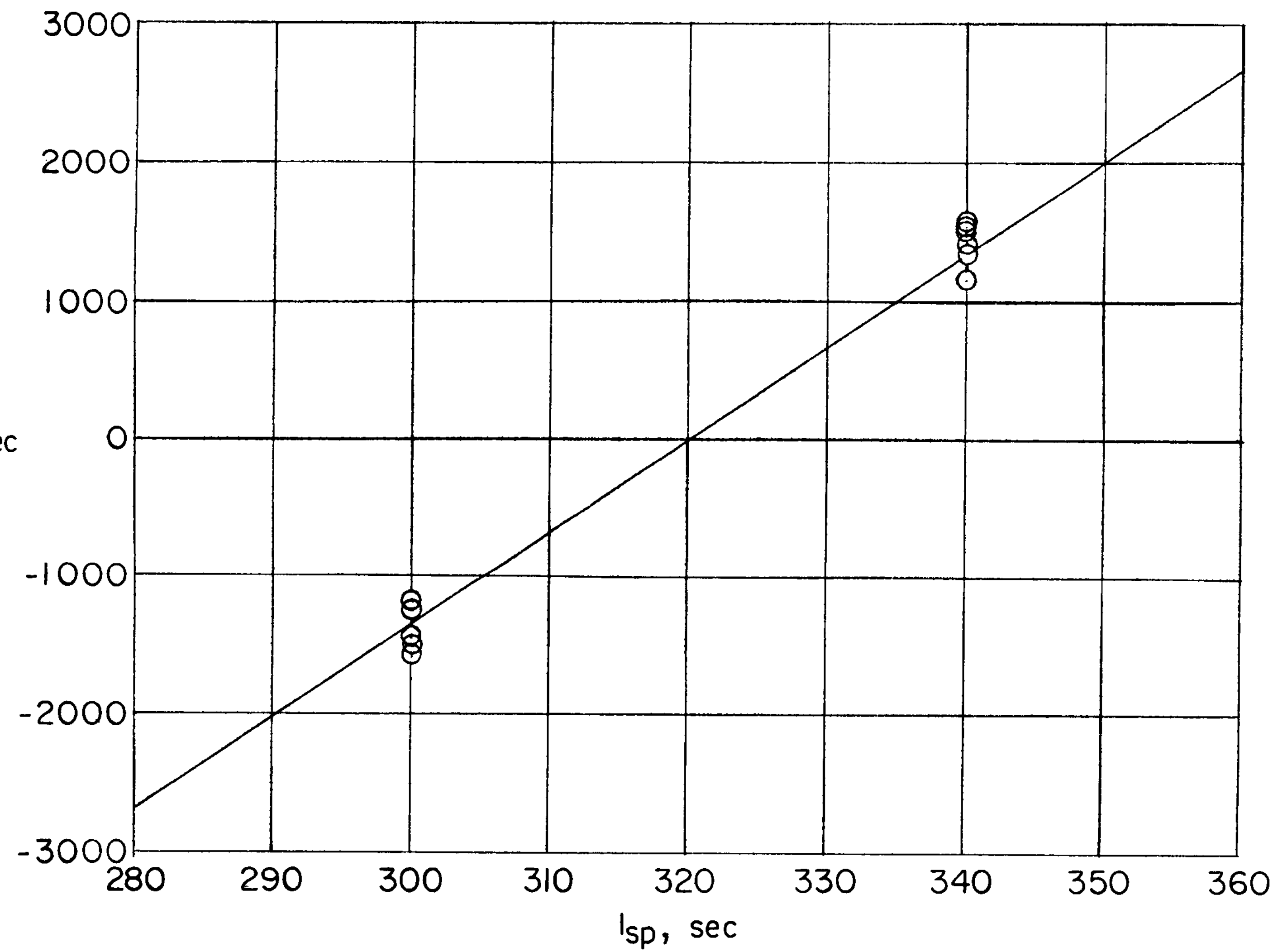

Figure 10.- Effect on burnout velocity of deviations in vacuum specific impulse from 320 seconds.

[redacted]

[redacted]

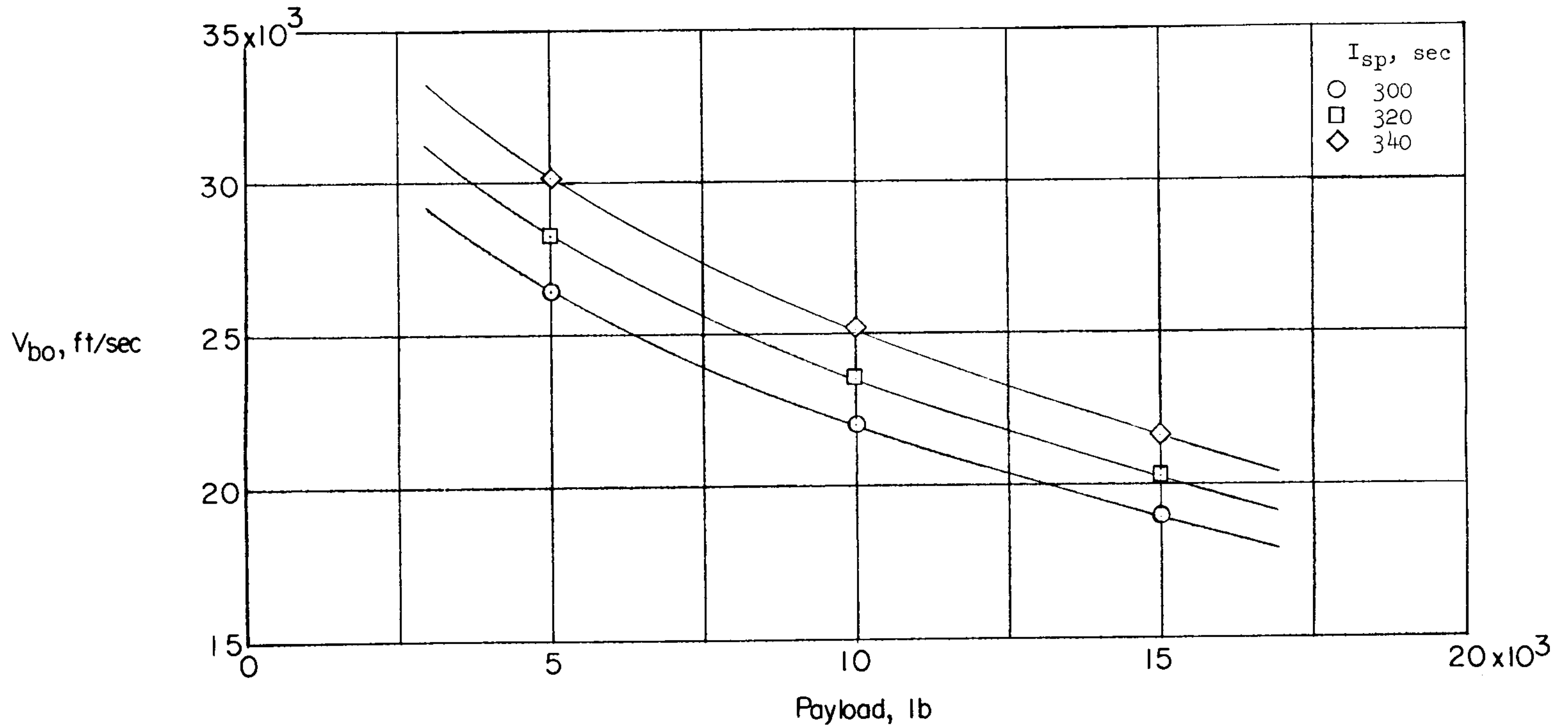

Figure 11.- Burnout velocities for various payload weights for a subsonic launch. Type C booster.

[redacted]

[redacted]

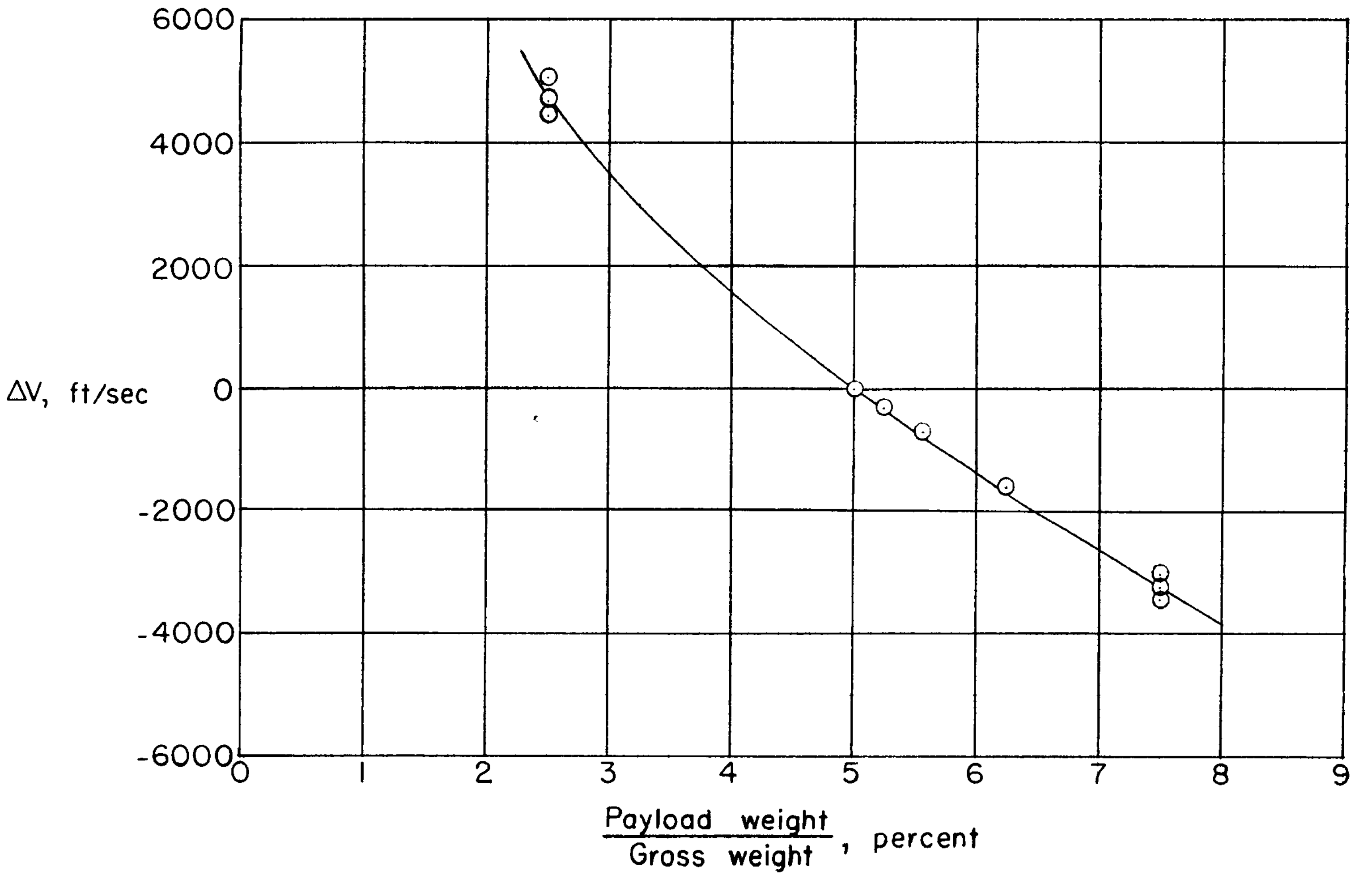

Figure 12.- Effect on burnout velocity of deviations of ratio of payload weight to gross weight from nominal value of 5 percent. Type C booster.

[redacted]

[redacted]

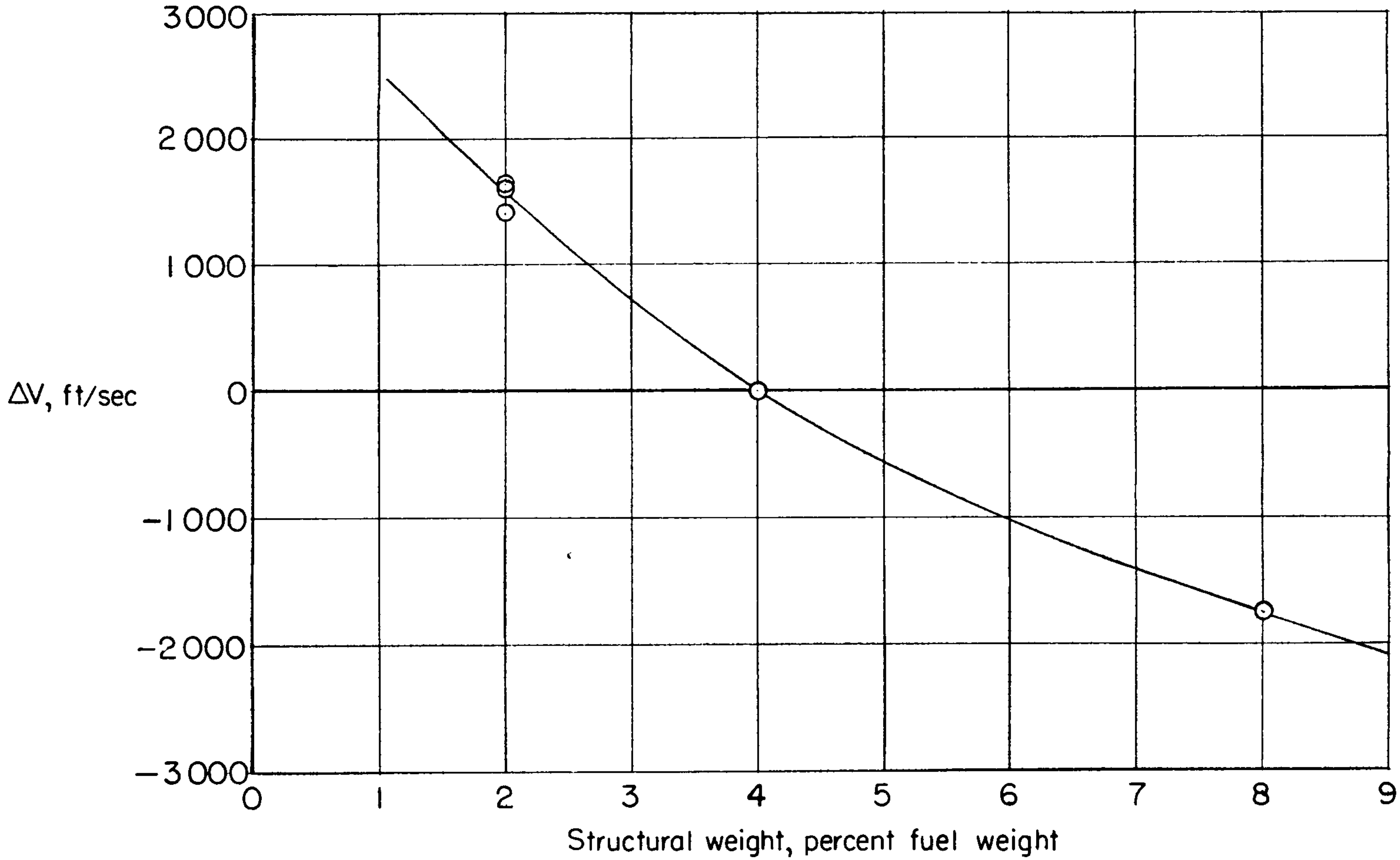

Figure 13.- Effect on burnout velocity of deviations in booster structural weight from 4 percent of the fuel weight.

[redacted]